Rethinking grounding-zone basal drag for improved projections of Antarctic ice loss

K. A. Hogan[1], J. A. Neufeld[2], C. Martín[1], M. Mas e Braga[1], A. M. Brisbourne[1], B. Kulessa[3], K. L. P. Warburton[2], J. D. Kirkham[1], O. J. Marsh[1], N. Holschuh[4], K. Christianson[5], J. Paden[6], C. Berndt[7], and R. D. Larter[1]

[1] British Antarctic Survey, High Cross, Madingley Road, Cambridge, CB3 0ET, UK
[2] Department of Applied Mathematics and Theoretical Physics, University of Cambridge, Wilberforce Road, Cambridge CB3 0WA, UK
[3] Glaciology Group, College of Science, Swansea University, Singleton Park, Swansea SA2 8PP, UK
[4] Department of Geology, Amherst College, Amherst, Massachusetts 01002-5000, USA
[5] Department of Earth and Space Sciences, University of Washington, Seattle, Washington 98195-1310, USA
[6] Center for Remote Sensing of Ice Sheets, University of Kansas, Lawrence, Kansas 66045, USA
[7] GEOMAR Helmholtz Centre for Ocean Research, Wischhofstrasse 1-3, D-24148 Kiel, Germany

Correspondence to: Kelly A. Hogan (kelgan@bas.ac.uk)

Emails addresses:

J. A. Neufeld (jn271@cam.ac.uk)
C. Martín (cama@bas.ac.uk)
M. Mas e Braga (mabrag@bas.ac.uk)
A. M. Brisbourne (aleisb@bas.ac.uk)
B. Kulessa (b.kulessa@swansea.ac.uk)
K. L. P. Warburton (klpw3@cam.ac.uk)
J. D. Kirkham (jamkir56@bas.ac.uk)
O. J. Marsh (olrs@bas.ac.uk)
N. Holschuh (nholschuh@amherst.edu)
K. Christianson (knut@uw.edu)
J. Paden (padenk@ku.edu)
C. Berndt (cberndt@geomar.de)
R. D. Larter (rdla@bas.ac.uk)

Manuscript Statement: This paper is a non-peer reviewed preprint submitted to EarthArXiv. This paper has not yet been submitted to a journal for peer review.

Abstract: Ice-stream grounding zones are critical parts of the Antarctic Ice Sheet and we must be able to model how they retreat with confidence. This is because for most of Antarctica, the grounding-zone location determines the flux of ice to the ocean. As such, future grounding-zone locations (as the ice-sheet edge retreats inland) dictate the pattern and rate of ice loss and the associated sea-level rise. Ice flow across the grounding zone is opposed by a combination of ice-shelf buttressing if lateral drag or pinning points are present, and by friction between the ice and its bed - basal drag. While the loss of buttressing and ocean-forced melting of ice shelves are popular research foci, far less attention is paid to resistance at the bed. Here, we revisit the treatment of grounding zones in models and argue for a new approach to basal drag: evolving bed conditions result in highly variable drag that is not captured by existing sliding laws. We begin by reviewing the complex basal processes operating in grounding zones over different timescales, such as tides, evolving subglacial hydrology, and sedimentation. Then, to illustrate the significance of the basal drag term, we run retreat scenarios in the UFEMISM model using an accepted basal sliding law that only varies in its treatment of subglacial hydrology (via effective pressure). Appreciable differences in retreat patterns motivate us to consider how modelling grounding zones may be improved. To reduce uncertainty in ice-loss projections, in tandem with refining ice-shelf melt parameterisations, careful observations from grounding zones and physically-based basal drag parameterisations are required.

1. Introduction

Mass loss from the Antarctic Ice Sheets (AIS) has trebled over the last 30 years, contributing to rising sea level, and potentially triggering a host of additional environmental tipping points (see Kubiszewzki et al., 2025; Antarctic and Southern Ocean only). Antarctic ice-sheet mass loss results from: (i) the flux of ice and meltwater across ice-stream grounding zones (GZs) and (ii) the retreat of ice-stream GZs leading to rapid flotation of previously grounded ice. Marine-based ice, such as in West Antarctica and many East Antarctic drainage basins, is vulnerable to GZ retreat because the ice sheet sits on a bed that is below sea level and deepens inland. This means that the further the ice edge retreats, the thicker the ice in the GZ and the higher the flux of ice to the ocean; in this way, retreat can become self-sustaining (Weertman, 1974; Thomas, 1979; Schoof, 2007; Vaughan & Arthern, 2007). Given this, knowledge of GZ locations and their retreat behaviour is essential to accurately predict future ice losses and associated contributions to sea-level rise because the GZ gateway controls the ice flux to the ocean (Schoof, 2007; Rignot, 2023; Parizek, 2024). However, ice behaviour in GZs is governed by complex interactions between the ice sheet, its bed, and the ocean which are notoriously difficult to observe because they occur beneath hundreds of metres of ice and ocean. This scarcity of observations is a real problem when trying to accurately simulate these complex regions and, therefore, is a barrier to improved predictions of their future retreat. In the words of Rignot (2023), GZs are “Achilles heel of the entire [Antarctic Ice Sheet] system” because there is such limited data with which to constrain this three-way boundary between ocean, ice, and bed in numerical models.

Much Antarctic research over the past decade has focussed on how warm ocean water is accessing and eroding the undersides of ice shelves in front of GZs, causing them to lose buttressing strength leading to the loss of upstream ice via ice-stream thinning and acceleration (Pritchard et al., 2012; Gudmundsson et al., 2013). Recent observations have revealed that the seaward edges of ice-

streams migrate farther than previously thought on short timescales with tidal forcing (up to 15 km from high to low tide positions over the course of 6 hours; Mohajerani et al., 2021; Chen et al., 2023); thus, these edges are not "grounding lines" but "grounding zones". Hence, we use the term grounding zone (GZ) in this paper unless describing a previously published grounding line with no width information. It is suggested that such GZ tidal motion could pump warm, salty water far upstream, melt basal ice, and ultimately force GZ retreat through the decoupling of ice from the bed (e.g., Milillo et al., 2019, 2022; Gadi et al., 2023; Rignot et al., 2024; Bradley & Hewitt, 2024). To account for uneven GZ retreat patterns even along individual GZs, these studies put forward the simple scenario that variable bed topography drives differences in GZ widths, dictating local retreat rates (Milillo et al., 2019, 2022). The argument is that ocean water intrudes further inland on retrograde slopes or via subglacial channels, whereas prograde slopes and high points in the bed block ocean inflows and provide local "pinning points", stabilising the ice by reducing flotation. At present, these arguments and follow-on model simulations of the so-called "melt-geometry feedback" (Bradley & Hewitt, 2024; De Rydt & Naughten, 2024) have little observational basis and tend to centre on how basal ice-shelf melting might be enhanced, with arguably less attention paid to processes at the bed that might influence the inferred decoupling (see, for example, Robel et al., 2022; Parizek, 2024).

However, we know that real GZs are far more complicated than these purely geometric models suggest. Numerous physical processes operate and interact across a range of timescales to modify the coupling at these ice-bed-ocean interfaces (Figure 1), a complexity that is fully recognised in recent forward-look papers (Parizek, 2024; Fricker et al., 2025). For ease of description, we use the collective term "GZ basal processes" to describe the physical interactions across the GZ. Each basal process influences the overlying ice dynamics by changing the coupling strength between the ice sheet and its bed; in other words, interacting basal processes change how ice slips over its bed, and so directly alter the resistive basal drag (Clarke, 2005). This is critical in ice-stream GZs where basal conditions are highly changeable (Fricker et al., 2025) meaning that the coupling strength, or basal drag, must also be highly variable over both space and time.

Let us consider the dynamical force balance for a GZ. The GZ position is determined by the vertical force balance or flotation criterion. The horizontal evolution of the GZ i.e., where the GZ repositions to during advance or retreat, is then determined by the flux of ice through the GZ as governed by the horizontal force balance (Figure 1). Ice-shelf extensional and driving stresses act to move ice to the ocean but are opposed by drag from the bed and lateral margins (Whillans & Van der Veen, 1997; Tsai et al., 2015). Lateral drag is explicitly calculated in higher-order models or is parameterised (e.g., Adhikari & Marshall, 2012) but it is unlikely to vary on distances less than one ice thickness (Schoof, 2002); buttressing by laterally-confined ice shelves has long been included in models (e.g., Dupont and Alley, 2005; Gudmundsson 2013). However, to accurately "locate" GZs in a model domain also requires knowledge of the basal drag term and, therefore, of the processes affecting it. GZ basal processes that are significant for basal drag include (but not are limited to): water ingress and outflow with tides (e.g., Horgan et al., 2013; Warburton et al., 2023; Rignot et al., 2024); episodic meltwater and/or groundwater release (e.g., Carter & Fricker, 2012; Horgan et al., 2025), the (re)configuration of the subglacial hydrological system (e.g., Schroder et al., 2016); bed geometry, roughness and composition (e.g.,

Christianson et al., 2016; Hogan et al., 2020); and bed elevation change via isostatic rebound (e.g., Larour et al., 2019; Book et al., 2022) or sedimentation (e.g., Alley et al., 2007; Bart et al., 2017).

In this paper, we focus on basal drag in Antarctic GZs because this is probably the most poorly constrained term of the force balance but also the most likely to evolve rapidly (Figure 1). We argue that GZ basal drag is inadequately represented in current sliding laws. We are specifically motivated by several research results. First, evidence from the much studied and vulnerable Thwaites Glacier (TG) indicates that GZ basal drag must have provided a significant backstop to outflow there because the ice shelf (of which now only the eastern part remains) had already lost much of its buttressing strength even >10 years ago (Parizek et al., 2013; Milillo et al., 2019; Robel et al., 2022; Schwans et al., 2023). Second, whilst noting the dependence of GZ retreat simulations on the basal sliding law that is used (cf. Brondex et al., 2017; Åkesson et al., 2021; Hank et al., 2025), multiple studies have also now demonstrated that GZ basal processes are important controls on retreat, and call for process-based and evolving parameterisations (e.g., tides: Warburton et al., 2023; subglacial drainage: Hager et al., 2022; bed rheology: Koellner et al., 2019; drainage and rheology together: Kazmierczak et al., 2024). Third, we remember an important GZ basal process that acts as a negative feedback on retreat and is currently missing from models: sedimentation (Alley et al., 2007). There is widespread evidence for more than 100 sediment wedges at past GZ locations around Antarctica that formed at the same time as decades- to centuries-long stillstands in deglacial ice retreat even in the face of strong regional climatic, ocean, or sea-level drivers (e.g., Ó Cofaigh et al., 2005; Bart et al., 2017, 2018). In the light of such overwhelming evidence in the geological record, and reinforced by modelling studies (Alley et al., 2007; Christian et al., *subm.*), we are motivated to explore GZ sedimentation further whilst noting its strong connection to the basal processes that impact basal drag, such as sediment and water transport, and bed roughness (cf. Alley et al., 2007).

2. Structure & Approach

The goal of this work is to demonstrate that basal drag in Antarctic GZs is a critical but uniquely difficult problem for ice-sheet models, and to determine how its representation could be improved. We naturally focus on the case of ice-stream GZ retreat. In this context, we aim to review Antarctic GZ basal processes, including sedimentation and wedge-building, drawing evidence from both modern (under the ice) and palaeo (on the continental shelf) GZ settings. In a second review section, we discuss the challenges associated with modelling Antarctic GZs and their basal drag. We then perform semi-realistic West Antarctic retreat simulations (real geometries, prescribed forcing) only varying the way subglacial hydrology is parameterised, to illustrate the effect of this basal process on retreat. We go on to consider how we might revise our approach to basal drag across GZs, using parameterised physics models capable of: (i) representing multiple complex physical interactions; (ii) of ingesting a wide range of observations; and (iii) of simulating both incredibly short (minutes-hours) and long (centuries-millennia) timescales. The latter two capabilities at least are currently outside the remit of most ice-sheet models.

3. Linking basal drag, sliding laws, and effective pressure

As this paper attempts to provide a bridge between those observing GZ processes and those modelling them, we begin with a brief introduction (including definitions) to basal drag, sliding laws, and effective

pressure as important concepts that we will return to later. For more information, the reader is referred to the vast scientific literature now available: see, for example Law et al. (2024) for a recent review.

Sliding Law	Key Idea	Main Equation	Typical Use	Reference
Weertman	Power-law sliding over hard beds	$u_b = C_W \tau_b^m$	Ice-sheet models without hydrology; hard beds	Weertman (1957)
Budd	Sliding depends on stress and effective pressure	$u_b = C_B \tau_b^m / N^q$	Glaciers influenced by water pressure	Budd et al. (1979)
Coulomb	Bed shear stress limited by friction	$\tau_b = CN$	Deformable sediments, soft-beds	Iverson et al. (1998)
Schoof	Includes Iken's bound induced by water-filled cavities	$\tau_b = \frac{C_s u_b^m}{\left(1 + \left(\frac{C_s}{C_{max} N}\right)^{1/m} u_b\right)^m}$	Fast flow with hydrological control	Schoof (2005, 2007)
Zoet-Iverson	Lab-derived sliding over water-saturated till.	$\tau_b = \mu N \left(\frac{u_b}{u_b + u_*}\right)^{1/p}$ $\tau_b = \min\left[N \tan(\phi), C\, u_b^{\frac{1}{m}}\right]$	Fast flow over deforming till	Zoet and Iverson (2020)

Table 1: A summary of the basal sliding laws most used in Antarctic ice-sheet models. N = effective pressure, τ_b = basal drag; u_b = basal ice velocity tangential to the bed; m, q and p, are the Weertman, Budd and Zoet-Iverson slip exponents ; C_W , C_B, μ, and C_S are the Weertman, Budd, Coulomb and Schoof friction coefficients; C_{max} is the Iken's bound, the maximum upslope angle of bed in flow direction; and u_* is a transition speed. C is also known as basal slipperiness in models. All sliding laws listed are used in ISMIP6 experiments (Seroussi et al., 2024).

Starting simply, to model ice flow we need to prescribe either the basal velocity (of ice), u_b, or the basal drag (at the bed), τ_b, the resistive force at the base of the ice that opposes its motion, or an equation, the basal sliding law, that connects the two, if both are unknown. Depending on the processes parameterised, different theories for the basal sliding law emerge; the main sliding laws used for Antarctica are summarised in Table 1, with their details in the references provided. For hard beds without lubrication or cavitation, based on the theory from Weertman (1957), it is assumed that basal drag and a power of the basal ice velocity are linked by a parameter commonly referred as slipperiness, *C* or *c*. In contrast, for fast-flowing ice that moves over a deformable bed of water-saturated sediments (till), the most common approach is to use a Coulomb sliding law (Iverson et al., 1998; Iverson & Iverson 2001). In this case, basal drag depends on the effective pressure *N*, which is the difference between ice overburden pressure and the subglacial water pressure:

$$N = p_i - p_w \qquad [3.1]$$

For intermediate cases (i.e., mixed bed types), there are sliding laws that combine Weertman and Coloumb-type flow, referred to as regularized Coulomb sliding laws (Schoof 2005, 2007; Gagliardini et al. 2007) and lab-derived sliding laws that describe the sliding over deformable beds (Zoet & Iverson, 2020).

It is clear from Table 1 that effective pressure (*N* hereafter) is an important variable for many sliding laws. Under an ice sheet, it is the hydrological system that sets the water pressure and, therefore, *N*. It is also known that basal drag is highly sensitive to *N* (e.g., Budd et al., 1979; Hank et al., 2025). These are almost canonical statements in glaciology now, but we argue here that *N* becomes even more critical, perhaps, in Antarctica's marine GZs. This is because the upstream hydrological system meets the ocean at this junction and, as such, water pressure varies in multiple ways across the GZ: (i) with distance across the GZ (scales of ~10s of kilometers) from nearly hydrostatic ocean values to a complex field in the inland subglacial hydrological system; (ii) along any given GZ (scales ~10^1-10^3 metres) according to variable bed composition, topography, and hydrological network; and (iii) across multiple timescales (~hours to centuries) according to the physical processes mentioned previously, such as tidal flexure, upstream meltwater release, and sediment deposition or erosion. Practical modelling of these GZs must, therefore, effectively parameterise an average of this variability in time and space, accepting the importance of *N* for basal drag and, in turn, of basal drag for predicting ice-sheet retreat using models.

4. Grounding-zone basal processes

It is commonly stated that GZ basal processes remain poorly constrained due to a paucity of observations. However, remote-sensing data and geophysical surveys have identified many processes, occasionally supplemented by point borehole and ROV observations (e.g., Powell et al., 1996; Christianson et al., 2013, 2016; Horgan et a., 2021, 2025). These "direct observations" are increasingly being acquired now that the significance of GZs is acknowledged, and new autonomous technologies enable their exploration (e.g., Schmidt et al., 2023; Calkin et al., 2025; Horgan et al., 2025). Regarding the distribution of Antarctic observations, the GZ of Whillans Ice Stream (WIS) on the Siple Coast, with its relatively benign surface conditions and ice-plain setting, is the most comprehensively studied, while scattered observations exist from a handful of other GZs.

To describe the complexity of real GZs (Figure 1) we take, in turn, the evidence for each basal process, and consider briefly their summative effect on basal drag by describing their influence on the bed and basal traction, often in terms of *N*. The basal processes are:

(i) water ingress and outflow with tides (hourly to fortnightly);
(ii) episodic water release and transient evolution of subglacial hydrology (daily to seasonal);
(iii) bed geometry, roughness, and composition (annual to decadal);
(iv) bed elevation change via isostatic rebound and/or sedimentation (annual to centennial).

4.1. Water ingress and outflow with tides. Although the concept of grounding line (GL) tidal migration has been around for many decades (Doake, 1978; Vaughan, 1995; Alley et al., 2007), the high repeatability and resolution of satellite datasets today (altimetry and interferometry) allow us to map the inland limit of ice-shelf flexure on hourly to daily timescales and, therefore, to measure GZ widths (Brunt et al., 2011;

Rignot et al., 2011). GZ widths range from a few hundred metres to multiple kilometres, and datasets have now been produced by machine-learning methods (Mohajerani et al., 2021) and released as bespoke data products, for example see the GL heat map published alongside the new Bedmap3 gridded data products using combined source data, and automated and manual methods (Pritchard et al., 2025).

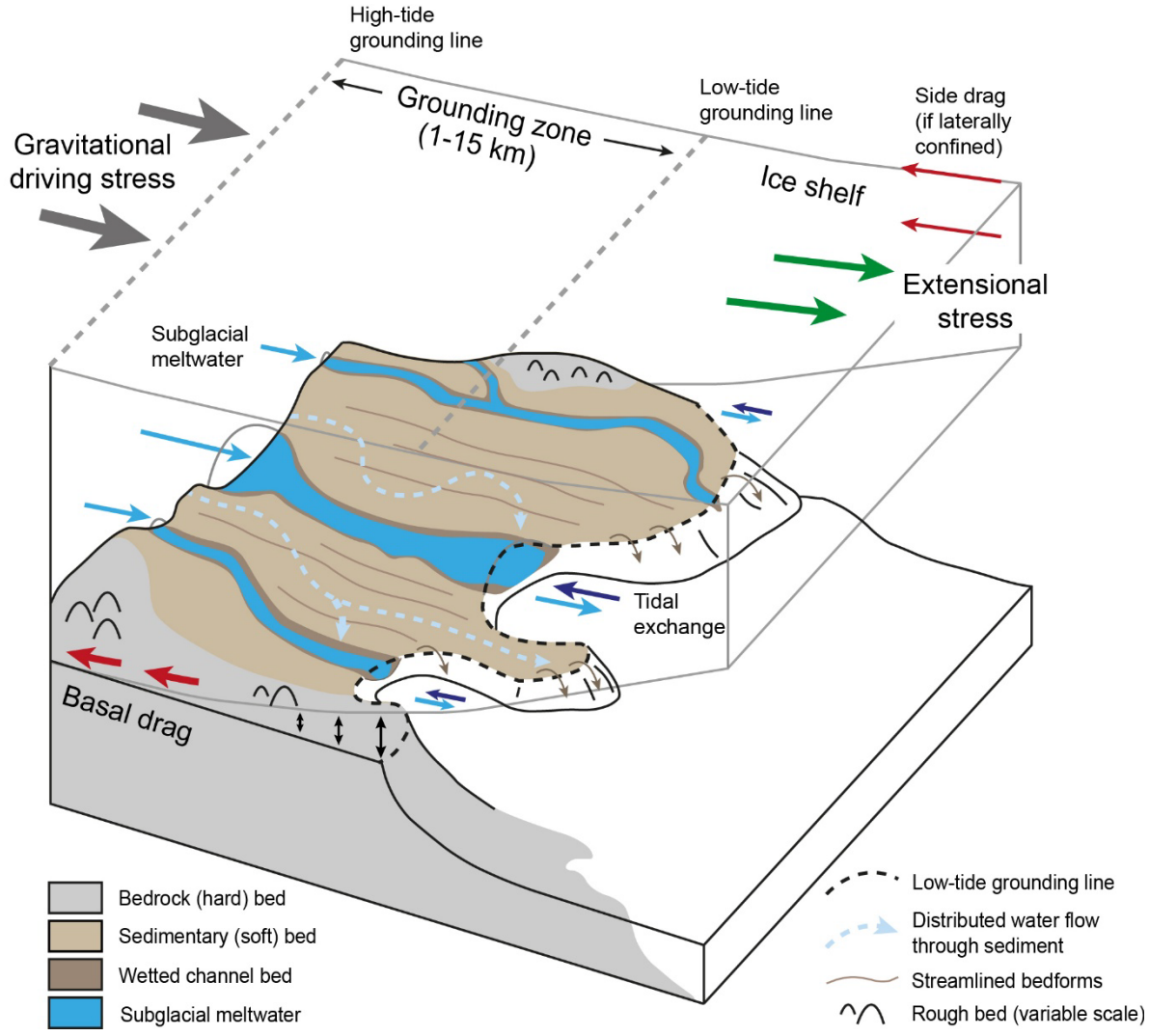

Figure 1: Schematic of an Antarctic grounding zone with the terms of the horizontal force balance. Basal drag acts against ice flow into the ocean and is affected by multiple interacting basal processes between the ice, the bed, and the ocean. They include the inflow-outflow of water, the roughness, geometry and composition of the bed, and the configuration of the local subglacial hydrology network, all of which vary across both short (hours-days) to long (centuries-millennia) timescales. Buttressing from the floating ice shelf is provided via side drag, if the ice shelf is laterally confined.

The opening and closing of a GZ cavity necessitates the ingress and outflow of seawater on tidal (hourly-daily) timescales, but the width of a given GZ depends on the local tidal amplitude, the bed topography, and the thickness and flexural strength of the overlying ice. The tidally-pumped seawater mixes with any freshwater emanating from upstream and that produced by local melting, leading authors

to describe GZs as tidal estuaries (Horgan et al., 2013; Fricker et al., 2025). Given the dynamics of the flow, it follows that the subglacial water pressure (and hence, *N*) will also vary with distance across the GZ on these timescales (Walker et al., 2013; Warburton et al., 2020), and therefore that the net effect of such water ingress and outflow must also depend on the local tidal forcing, the geometry of the GZ cavity, the composition of the bed, and the degree of ice melt across the GZ. If ice-shelf melt is occurring in the GZ, inflowing (warm) ocean water will spend less time in contact with the ice further upstream than at the low-tide GL position, and can be expected to lose some of its heat as it intrudes, becoming less potent upstream.

It is not feasible to measure *N* directly, so we rely on models to test how tidal changes affect sliding over the bed via time-varying basal drag. For example, Walker et al. (2013) modelled ice-shelf flexure with the GZ pinned at a stationary point (non-migrating GL) and found that ice stream GZs may draw water in during rising tides, forcing it further inland when the subglacial pressure gradient switches back to a falling tide. Changes in water pressure resulting from this "gulping" mechanism would inevitably change the basal lubrication (i.e., by either increasing or reducing the basal drag) at least locally, although the authors clearly state that the pervasiveness and form of the change depends on the detailed structure of the hydrological system and composition of the bed. More recently, Warburton et al. (2020) considered the case of an unpinned GZ that migrates over the tidal cycle. Their model incorporated higher resistance to water flow inversely proportional to the distance between the ice and the bed, and hence the GZ moves rapidly during the rising tide with water draining slowly from the GZ during the falling tide. This remnant water lubricates the GZ, lowering the basal drag. Further modelling of water flow in GZ cavities has returned a wide range in possible seawater intrusion distances (up to several kilometres) but these studies caution that the form and extent of such intrusions are highly dependent on the geometry of the bed and of the ice base, as well as bed composition, and that all of these GZ basal characteristics require further constraint by observations (Wilson et al., 2020; Robel et al., 2022; Mamer et al., 2025).

4.2 Episodic water release and the subglacial hydrological system. Enhanced subglacial water flow across any GZ will alter the lubrication or slipperiness of the bed depending on the configuration of the hydrological system. Efficient drainage in channels reduces water content at the bed and increases basal drag, whereas inefficient drainage through till, typically represented with porous Darcian flow, provides lubrication and reduces basal drag (Clarke, 2005). We know from the recent satellite record that "active" subglacial lakes under Antarctic ice streams have drain-and-fill cycles on ~annual to multi-decadal timescales (Malcyzk et al., 2020; Wilson et al., 2025). However, we do not yet know whether or how this water propagates downstream and across the GZ, although hydrology models predict this propagation, and there are observations of correlated ice speed-up events at the GZ (e.g., Carter & Fricker, 2012; Miles et al., 2018; Gourmelen et al., 2025). As a counterpoint, a recent study at WIS showed that drainage of a subglacial lake and subsequent retreat of the GZ nearby were unrelated events (Freer et al., 2024). On longer timescales (centuries-millennia) and based on extensive channel networks eroded into hard bedrock, subglacial lakes under ice streams during the Last Glacial Maximum and deglaciation have been predicted to fill (and so potentially drain) on predominantly multi-year to centennial timescales (<1-2600 years) but with considerably higher peak water fluxes (500 $m^3 s^{-1}$ versus 10 000 $m^3 s^{-1}$; Wingham et al., 2006; Hogan et al., 2023). These high peak fluxes are required to erode crystalline bedrock and can

be achieved if subglacial lakes drain in a cascading way through connected networks along ice-stream pathways (Kirkham et al., 2019; Hogan et al., 2023). Presumably, the water is eventually expelled at GZs at the ice-sheet margin.

Despite these differences in the frequency and flux of episodic water release, there is certainly convincing observational evidence of large (up to 100s m wide and high) subglacial R-channels (eroded up into the ice) crossing modern ice-sheet GZs, and persisting year-on-year and for 100s of kilometres upstream (Le Brocq et al., 2013; Alley et al., 2016; Drews et al., 2017; Hofstede et al., 2020; Dow et al., 2022). Models suggest that subglacial drainage through such GZ channels enhances ice-shelf basal melting, especially when a buoyant plume forms (Nakayama et al., 2021; Gwyther et al., 2023; Cheng et al., 2024), a process that is now widely accepted (Parizek, 2024) and recently backed-up by observations (Whiteford et al., 2022). Large, episodic drainage events such as those modelled during the last deglaciation must also have the potential to flush out the GZ cavity, temporarily overwhelming the hydrological system and reducing basal drag. Furthermore, such "floods" could mobilise sediments across the GZ (e.g., McMullen et al., 2006; Simkins et al., 2018) or even erode channels into bedrock (see calculations and discussions in Kirkham et al., 2019 and Hogan et al., 2023), vastly changing the local bed conditions in terms of bed composition, roughness, and water content. As such, these temporary flood events may even "reset" GZ basal conditions on a semi-regular, albeit longer-timescale, basis.

Deep groundwater is another less well understood component of the subglacial water budget under ice streams (see Siegert et al., 2018 for a review). The development, and increasing deployment, of electro-magnetic (EM) instruments alongside seismic methods at Antarctic ice streams is revealing the distribution of groundwater in regional sedimentary basins, as well as potential movements between this bedrock and the subglacial till that lubricates fast ice flow. In GZs, the interest is in how groundwater interacts with seawater and such EM methods may be used to confirm how far inland low resistivity seawater pervades on, for example, tidal timescales (Key & Siegfried, 2017). One combined EM and seismic survey at WIS has delineated a 1-km thick sedimentary unit beneath the GZ containing significant groundwater that is salt stratified (i.e., freshest at the top and increasingly saline with depth; Gustafson et al., 2022). The authors speculated that the deep saline porewaters may have been trapped in subsurface sediments during a phase of Holocene retreat or were left over from the original deposition of the marine sediments. Freshening of the uppermost sediment porewaters was interpreted as infiltration of meltwater from the ice base, through subglacial till, and into lithified sediments suggesting connection between the "shallow" (meltwater plus till) and "deep" (groundwater) hydrological system.

The effect of groundwater on GZ basal drag is not yet known as only a few studies exist (e.g., Cairns et al., 2025). However, it presumably depends on the composition and structure of the bed, and the dynamics and timing of previous ice advances, and of current ice retreat. Ice-stream thinning close to a retreating GZ would reduce the load on the bed and could enhance water drawdown (fresh melt or saline ocean or a mixture) akin to a sponge under pressure sucking up water when compression is released. Such a feedback would, in theory, enhance lubrication at the bed. Again, the exact effect on basal drag would likely depend on the distribution and thickness of subglacial sediments, the rate of infiltration (related to retreat dynamics), and the geometry of the GZ cavity and ice base.

4.3 Bed geometry, roughness and composition. Variability in GZ bed geometry occurs across a range of spatial scales, from kilometre-scale embayments and topographic highs on the bed to metre-

decimetre scale roughness that changes with bed composition (most often categorised as hard, soft or mixed bed types under Antarctica) and the occurrence of subglacial landforms or geological structures (see Alley et al., (2021) for a recent discussion). At broad multi-kilometre scales, the geometry of Antarctic GZ beds vary from near-flat, often smooth beds in ice-plain settings such as in WIS (Christianson et al., 2016), to rough beds with bedrock ridges lying perpendicular to ice flow such as at TG (Figure 2a, 2c) (Holt et al., 2006; Jordan et al., 2023). Flatter beds tend to be composed of sediment and thus are inherently smoother and prone to low basal drag and fast sliding (Arthern et al., 2015). However, as noted previously, a flat or inland-deepening bed (on kilometre-scales) both increases the degree of tidal exchange and basal ice melt by vigorous water flows (e.g., Milillo et al., 2019, 2022) and increases the ice thickness and ice flux during GZ retreat. This set-up acts to reduce basal drag as ice decouples from the bed. In contrast, beds that shallow inland across the GZ will have decreasing GZ thickness during retreat, reduced tidal exchange, and will tend to promote a stable GZ position as the ice flux lessens as the GZ retreats, and the likelihood of flotation decreases (Vaughan & Arthern, 2007; Alley et al., 2007). Observations show that some flat or inland-deepening Antarctic GZs have pronounced high points within their GZs that appear to have a stabilising effect on the GZ position (accepting that stability can also be dictated by ice-shelf side drag, see Figure 1). This is the case for the GZ of Institute Ice Stream where airborne radar has revealed a 100-m high “bump” in the overall bed thought to be a stabilising influence (Siegert et al., 2016). Similarly, at WIS, the GZ is pinned at a pronounced ~30 m high pinning point which the GZ wraps around (see the “peninsula area” in Figure 2b).

An example of a rough-bedded GZ pinned on a bedrock sill is the Thwaites GZ. Mapping shows it has a highly sinuous form that is largely governed by km-scale highs and lows on the bed (Figure 2a) (Rignot et al., 2014, and see Figure 1B in Milillo et al., 2019). The sinuosity has increased over time as the GZ has retreated further within the topographic lows or embayments. As well as raising the ice out of the water, high points in the bed are probably characterised by small-scale (m to 100s of m) roughness as they typically comprise bedrock. Thus, topographic highs are associated with slower sliding over the bed (Arthern et al., 2015; Hogan et al., 2020; Alley et al., 2021). Recent progress in how we translate measured 3D bed roughness on metre-scales (10s to 100s of m) into form drag, or resistance to ice motion (see Hogan et al., 2020 and Hofmann et al., 2022, after Schoof, 2002), confirms that the roughest regions of the bed (i.e., geological structures or subglacial landforms) do indeed provide the most resistance to flow. However, the effect of finer-scale roughness on metre to sub-metre scales is not yet resolved. This could be a controlling factor on basal drag if the relationship between the frequency of bed topography and form drag holds for these smaller scales (Hogan et al., 2020; Hoffman et al., 2022). Of note, perhaps, is another conclusion of Hoffman et al. (2022), that fine-scale bed roughness around a subglacial lake appeared to be more important to local basal drag than changes in N associated with a lake drainage event. This means that, at least sometimes, bed roughness may dominate the basal drag budget over changes in N, a point that is highly relevant for GZs which experience changes in both roughness and N across a range of length- and time-scales.

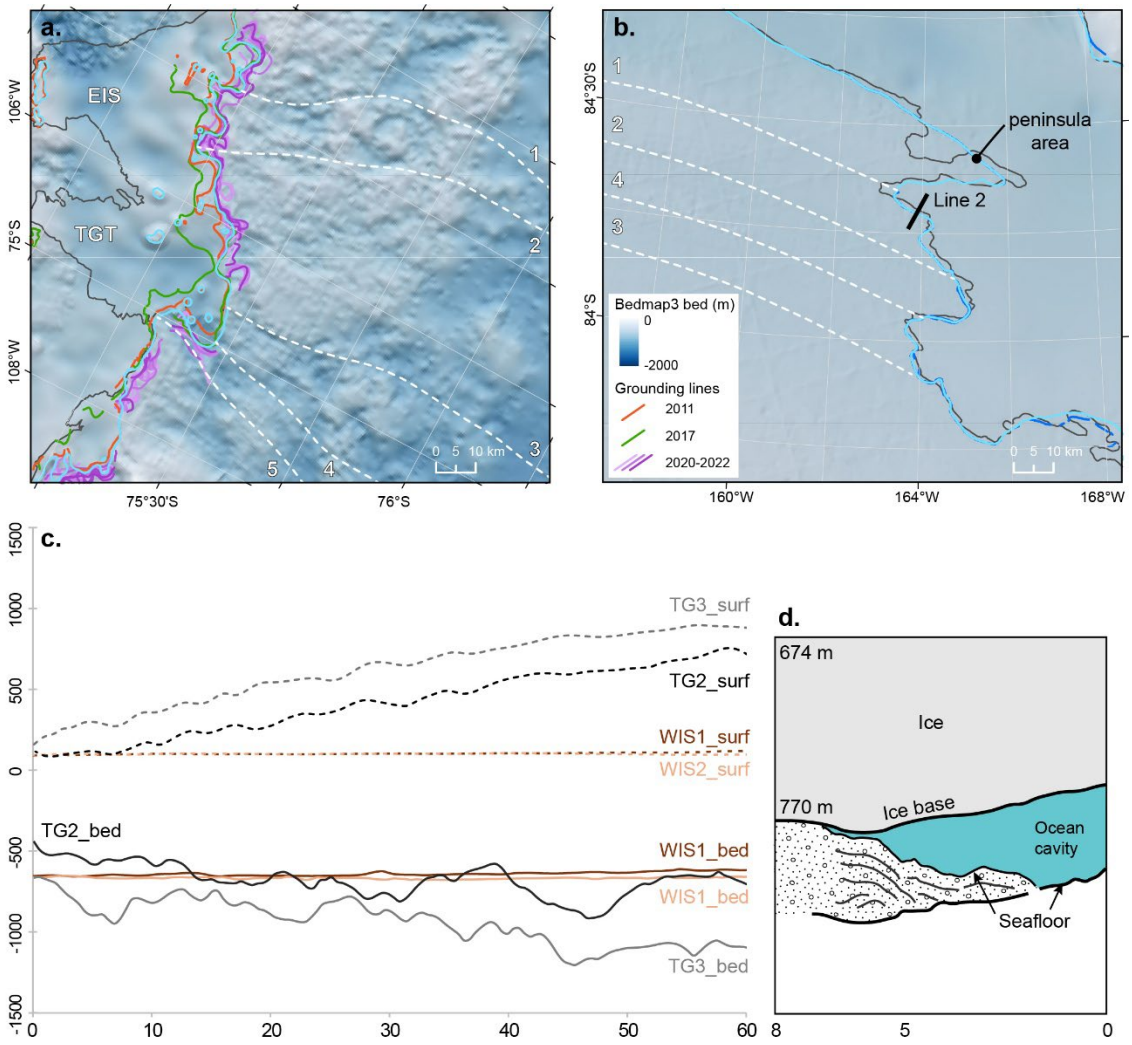

Figure 2: Some bed characteristics of two modern marine grounding zones. The mapped grounding lines and bed topography from (a) Thwaites Glacier (TG), and (b) Whillans Ice Stream (WIS). (c) Surface and bed profiles for two flowlines (derived from BedMap3 and labelled in (a)) from TG and WIS showing the rough bed at TG, known for its mixed bed type, and the very smooth bed at WIS in its ice-plain setting. The GZ of TG which is known to have high basal drag has evolved to be more sinuous over time on scales of a few kilometers with faster retreat within small embayments adjacent to topographic highs. Bed topography and profiles are from Bedmap3 (Pritchard et al., 2025). (d) Line drawing of a seismic-reflection profile with depths (calculated from velocities in ice) from Horgan et al. (2021) across the WIS GZ (location in (b)) showing prograding sediment units upon which the GZ is effectively pinned.

4.4 Bed deformation via GIA and sedimentation. Both glacio-isostatic adjustment (GIA) in response to ice mass loss and active sedimentation in ice-shelf cavities have the potential to raise bed elevations in Antarctic GZs (as well as in upstream areas for GIA). By reducing the degree of flotation or increasing the height (of ice) above hydrostatic equilibrium these processes can forestall GZ retreat (Pattyn and Morlighem, 2020). However, the two processes operate on different timescales. Simulations including GIA confirm that this process slows ice-sheet decay on centennial timescales (Larour et al., 2019), whereas it is not yet clear how important the more immediate elastic GIA response over ~decades is. In

contrast, our understanding of sedimentation at ice-sheet GZs from the palaeo-geological record is that thick wedges of sediments (10s to 100s m thick) can build-up on timescales of decades to centuries during phases of sustained GZ retreat (Dowdeswell & Fugelli, 2012; see also Section 4.5). Growth of these grounding-zone wedges (GZWs) can enable an ice-stream GZ to remain stationary at that location, or even cause small readvances, while the ice above the GZ is gradually thinning for several centuries to millennia as long as the high sediment flux continues (Bart et al., 2017).

Spatially, it is notable that the more vulnerable West Antarctic Ice Sheet (WAIS) is underlain by a weak Earth structure (low-viscosity asthenosphere, thin lithosphere) and so experiences faster and more localised GIA uplift than other regions (Barletta et al., 2018). Those authors found that even if they simply maintained present-day ice-thinning rates and did not increase them, the GZ of Pine Island Glacier would rise up by 8 m in 100 years. Thus, GIA could be an effective mechanism for slowing GZ retreat on decadal timescales at least in some parts of Antarctica. For GZ sedimentation to rapidly build an effective wedge (i.e., spatially-extensive and raises the bed fast enough to counterace ice-shelf melt forcing) requires a ready source of sedimentary material from upstream. Antarctic ice streams are associated with flow over soft tills via sediment deformation (Kamb, 2001) *ergo* sediments should be available to move to ice-stream GZs. A recent map of Antarctic sedimentary basins, compiled from geophysical datasets and ML methods (Aitken et al., 2024), revealed that many ice streams are indeed underlain by sedimentary basins in their lower catchments providing a ready supply of erodible sediments to GZs (e.g., Siple Coast ice streams; Institute, Academy, Support Force in the Weddell Sea area; and Jutulstraumen, Ragnhild and Cook in East Antarctica). The authors go on to confirm that even ice streams that have eroded through older marine sediments in their lower catchments, and so flow over hard or mixed bed types (e.g., Pine Island, Thwaites, Recovery, Slessor, Lambert, Mellow, Denman, Scott, Totten), still rest on some thickness of unlithified till at the bed, as indicated by low basal drag that extends far upstream. This suggests that sediment supply is probably not a limiting factor on GZW build-up for most Antarctic ice streams.

The simple occurrence or redistribution of sediments in a GZ, or changes in the sediment properties, will alter basal drag locally (Whillans & Van der Veen, 1993; Alley et al., 2007; Iverson et al., 2010). Stiffer tills increase drag, weaker tills will reduce it. An easy analogue for spatially and temporally variable basal drag resulting from dynamic sediment changes are, perhaps, ice-stream sticky spots located at patches of “stiffer” till, and common under the Siple Coast ice streams (e.g., Stokes et al., 2007; Leeman et al., 2016). At WIS, sediments just inland of its GZ are compacted and dewatered by ice-sheet flexure (Christianson et al., 2016; Hofstede et al., 2021; Horgan et al., 2021) and increase the basal drag (Walker et al., 2013). This mechanism probably stabilises the WIS GZ in the absence of positive topography along most of its GZ (Figure 2b). Furthermore, seismic stratigraphy in one embayment indicates that, despite limited accommodation space, *prograding sedimentation*—the outward growth of sediment layers into the basin—is likely occurring. This is shown by the downlap and toplap of reflections on seismic profiles just below the ice base (Figure 2d; Horgan et al., 2021). Beneath these prograding units, chaotic reflections are interpreted as subglacial tills, the deposition of which may have locally enhanced drag and promoted the initial pause of GZ retreat at this location. A step in the seafloor bathymetry here is interpreted as the active front of a sedimentary lobe, although there is no evidence of a high-profile (10s-

100s m high) sediment wedge having accumulated. This recent or ongoing sedimentation is interpreted as the direct cause of observed ephemeral grounding in the embayment (Horgan et al., 2021).

Moving to the Weddell Sea sector, at the Support Force GZ, downstream of a basal channel, Hofstede et al. (2021) observed a 200-m thick sedimentary deposit 6.75 km long and 3.2 km wide on seismic reflection profiles. Weakly-stratified internal reflections, some dipping seawards, led the authors to interpret the deposit as a grounding-line fan (cf. Powell, 1990; Dowdeswell et al., 2015). Such fans form as subglacial material is extruded from the meltwater channel and deposited on the seafloor by gravity flows. In another example, actively evolving, large eskers (sediment ridges, ~250 m high, sedimentation rates 1.4 m a^{-1} over 175 years) found in subglacial channels in the GZ of West Ragnhild ice stream (Roi Baudouin Ice Shelf, East Antarctica; Drews et al., 2017) are strong evidence for: (i) water flow through such channels transporting sediment to GZs (Horgan et al., 2013); and (ii) sedimentation changing the GZ geometry on decadal timescales. Such observations of active sedimentation at modern GZs demonstrate that the composition, geometry, and therefore basal drag, of GZs must evolve as the sediment distribution evolves. We go on to consider the geological record of grounding-zone wedges (GZW) separately below.

4.5 Grounding-zone wedges - an understudied negative retreat feedback? Almost 30 years of work on sedimentary GZWs has shown a strong association of sediment build-up with long stillstands (decades to millennia) of individual ice-stream GZs (e.g., Anderson, 1999; Ó Cofaigh et al., 2005; Dowdeswell & Fugelli, 2012; Bart et al., 2017, 2018). Modelling experiments confirm that, once initiated, GZW build-up extends slowdowns in retreat into sustained stillstands (Alley et al., 2007; Christian et al., *subm.*). Despite these results, GZ sedimentation - or put another way, bed geometry evolution - is not included in ice-sheet models in any form. This is contrary to the attention now being paid to the ice-shelf geometry feedback (cf. Bradley & Hewitt, 2024; De Rydt & Naughten, 2025). As mentioned above, and despite a growing body of observational evidence, questions persist about the processes and rates of sediment transport to and deposition across modern GZs, ultimately leading to the question: can GZWs be built around Antarctica today and provide a negative feedback to ongoing rapid retreat? A major hurdle to this idea seems to be the discrepancy between high palaeo-sediment fluxes (to GZWs) versus the subglacial flux estimates for the present-day ice sheet. Here, we attempt to clarify these issues by providing a selective review of GZWs, linking ideas from recent research and our own thinking.

GZWs are asymmetric wedges of heterogeneous subglacial till and sediment gravity flows that extend across ice-stream pathways. More than 100 examples have now been described from 22 glacial troughs around Antarctica (Figure 3) (n = 103; Batchelor & Dowdeswell (2015) and updated by us). GZW geometries are strikingly similar: wedges are <15 km long (along ice-flow), 10-100 m thick, have upstream slopes of 0.01-1°, and downstream slopes of 1-10°. Due to their angular similarity, the low upstream slopes are assumed to reflect the base of low-angled ice shelves with sedimentation occurring in limited accommodation space (Dowdeswell & Fugelli, 2012). Although neither proven nor disproven by a recent modelling study (Christian et al., *subm.*), we reiterate the observation that no GZWs are reported from the seafloor adjacent to the many tidewater glaciers found across the Arctic (although moraine ridges have formed) suggesting that ice shelves are indeed necessary to produce GZWs. In fact, the development of sedimentary bodies with “GZW” geometries at GZs beneath ice shelves was

hypothesised by Alley et al. (1986, 1987, 1989) before any such deposits had been identified. Nevertheless, when paired with well-dated sedimentary records, GZWs have been shown to mark former GZ and ice-shelf locations, produced during stillstands lasting ~a few decades to 1-2 millennia (e.g., Ó Cofaigh et al., 2005; Bart et al., 2017, 2018; Roseby et al., 2022). The paucity of examples from East Antarctica (see Figure 3) is due to a lack of seafloor data in these areas rather than the absence of wedges, and we assume that the scarcity of observations from modern GZs is at least partly responsible for the lack of "modern" wedges. For now, we know of two GZWs reported from modern GZs at WIS and TG, respectively (Figure 3) (Anandakrishnan et al., 2007; Schmidt et al., 2023).

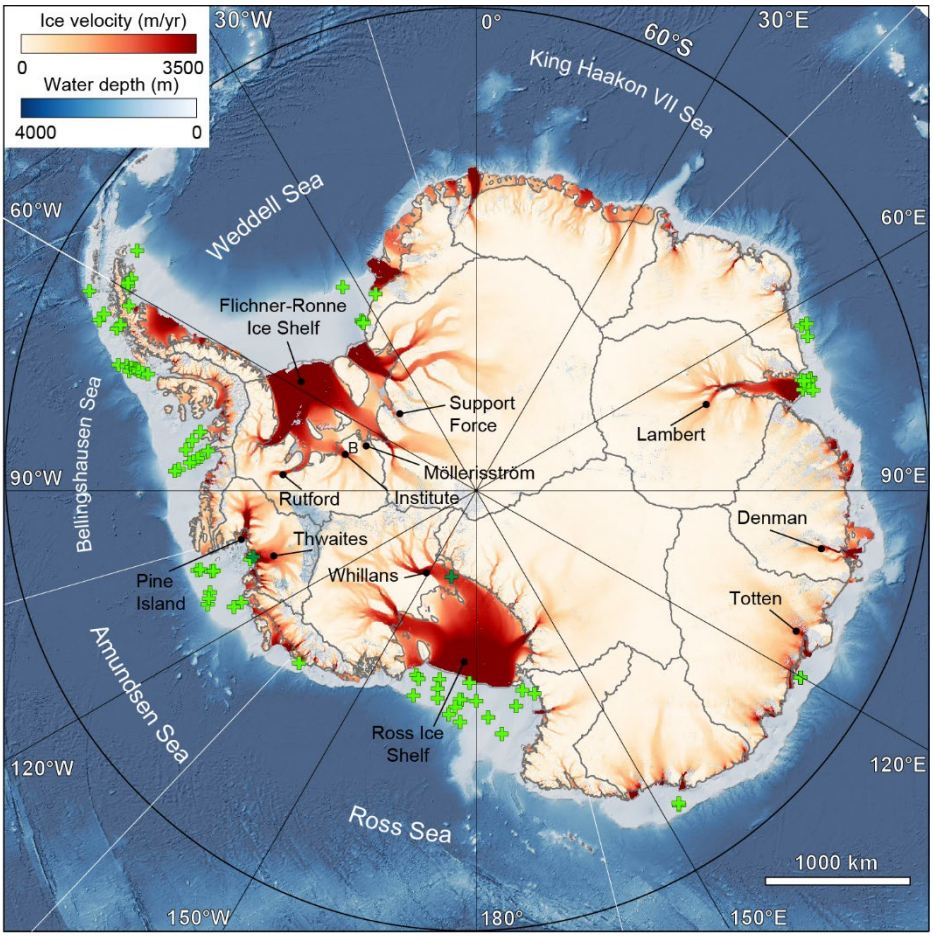

Figure 3: Antarctic ice velocities (MEaSUREs V2; Rignot et al., 2017) showing the fast-flowing ice streams that terminate in marine grounding zones and the sedimentary grounding-zone wedges (GZWs; green crosses) found around Antarctica. Dark green crosses are GZWs observed at present-day grounding zones. Labels locate the ice streams discussed in the text; B is the Bungenstock Ice Rise; drainage basins are derived from Bedmap3 (Pritchard et al., 2025); bathymetry is from IBCSO V2 (Dorschel et al., 2022); wedge locations are from Batchelor & Dowdeswell (2015) and updated by us.

Multibeam bathymetry and seismic profiles that image seafloor GZWs elucidate the physical processes associated with their formation. Internal reflections dipping down to the seaward toe of the wedge (e.g., Blakenship et al. 1989; Larter & Vanneste, 1995; O'Brien et al., 1999; Dowdeswell and Fugelli, 2012; Bart et al., 2017) plus surface features of down-slope sediment movement (e.g., Bjarnadóttir et al.,

2013) provide compelling evidence for sediment deposition by gravity flows on wedge fronts. The mechanism of sediment build-up is shown in Figure 4. Once accumulation begins, sediment builds upwards and in a seaward direction at the same time, meaning that as individual subglacial till units are emplaced, the GZW can also prograde forwards over sediments that have been redeposited from the gravity flows. Subaqueous down-slope flows are known to occur on extremely low slopes (<2°), often attributed to rapid accumulation rates and high excess pore water pressures (e.g., Urlaub et al., 2015), thus providing an explanation for the low frontal angles of GZWs. The result of this pattern of build-up, during phases of sea-level rise, is that the GZ front migrates (advances) in a seaward direction while its surface may grow higher as the wedge develops (Figure 4). Other important observations from GZWs are the identification of v-shaped channels within some GZWs, or on their surfaces, that are 100s to 1000s of metres wide and 10s of metres deep (McMullen et al., 2006; Dowdeswell & Fugelli, 2012). The incised channels are not topographically controlled so are interpreted to be the result of high-pressure meltwater flow within subglacial channels across these former GZs.

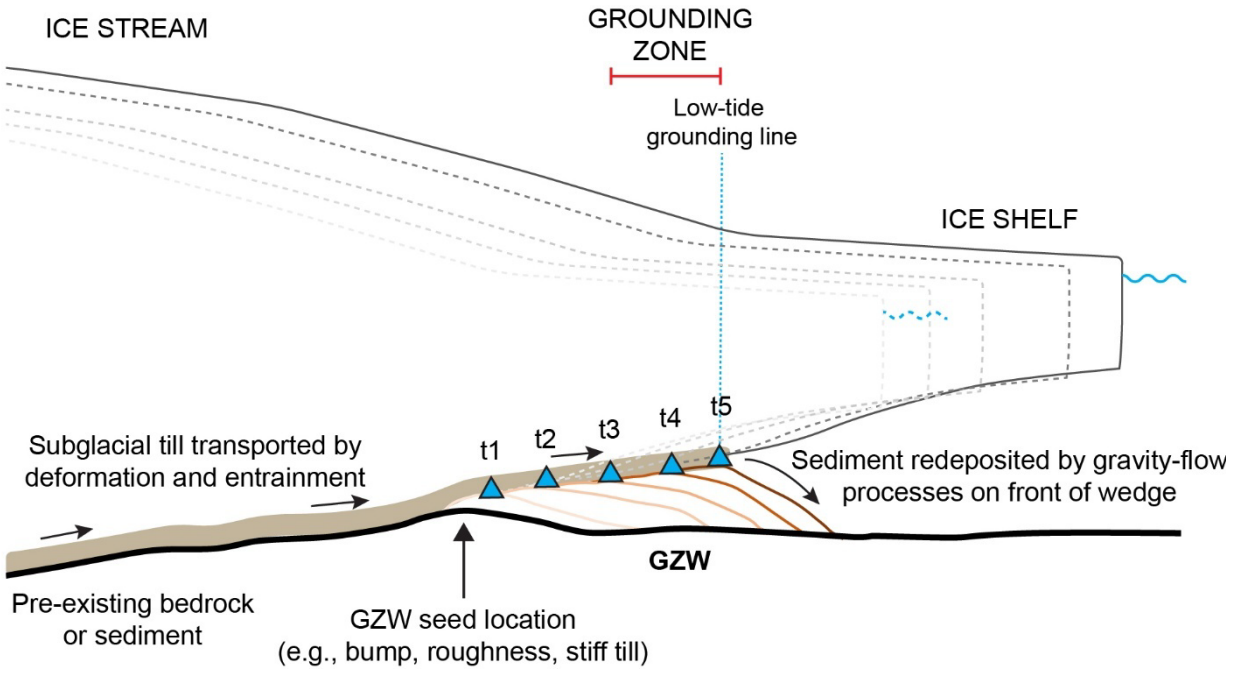

Figure 4: Schematic model of grounding-zone wedge (GZW) formation during a period of sea-level rise. Sediment transport under the ice can occur either by sediments moved in a deforming layer or by material entrained into basal ice. No matter the transport mechanism the internal structure of GZWs, known from seismic profiles, identifies that they form by sediment being delivered to a seed location and then the wedge builds upwards and seawards with each time-step thereafter (i.e., moving from t1 to t5). Although some GZWs have seed locations associated with a topographic feature (either a bump in the bed or a narrowing of the glacial trough), many do not; in B&D (2015) only 18% of the GZWs are associated with a topographic feature on the bed.

We turn to the discrepancy between modern and palaeo subglacial sediment fluxes. Fluxes under the modern ice sheet (~10s of $m^3m^{-1}a^{-1}$; units are cubic metres per metre of ice-stream width per year) are inferred from indirect observations of sediment content and its fabric (in ice) , from boreholes, and by making assumptions based on glaciological theory. In contrast, fluxes in the palaeo record (~10^3-10^5 $m^3m^{-1}a^{-1}$) are calculated from the volume of GZWs or other ice-marginal deposits plus well-dated ice-retreat histories to constrain the period of deposition. We compile the available estimates for all subglacial sediment fluxes in Table 2, stating the method by which the flux was calculated. We note that modern fluxes are often calculated from locations upstream of GZs and may not necessarily be indicative of sediment extrusion at the GZ. Most modelling papers to date have used the low modern flux rates in their calculations, which has resulted in estimations of long build times for GZWs. For example, experiments in Christian et al. (*subm.*) took 2000 years to build a relatively small wedge (10-20 m thick).

We can use the best known and largest Antarctic GZW discovered to date to further explore the sediment flux conundrum. The Whales Deep GZW (~90 km wide, >100 m high; total volume: 5.34 x 1011 m^3, Bart & Tulaczyk, 2020) is a composite wedge with at least seven stacked units (equivalent to seven phases of deposition) laid down on top of each other at a former GZ of the palaeo-Bindschandler Ice Stream (BIS) during deglaciation (Bart & Owolana, 2012; Bart & Cone, 2012; Bart et al., 2017, 2018; Bart & Tulacyzk, 2020). Comprehensive geophysical surveying, sediment coring and radiocarbon dating of the wedge shows that it formed over a period of ~2300 years, straddling a period of significant ice-shelf break up. This is important because the wedge continued to build, and the GZ remained stable at that location, for ~1000 years after the ice-shelf collapse (Bart et al., 2017). Such a pattern of stability without an ice shelf is somewhat contrary to the current paradigm that the loss of ice-shelf buttressing is the dominant control on ice-stream retreat (e.g., Gudmundsson, 2013; Rignot, 2024).

Ice stream	**Sediment flux, *Q* (m^3 m^{-1} a^{-1})**	**Evidence / Methodology**	**Reference**
Palaeo-Bindschadler IS	4.7×10^8 (max.) 1.7×10^8 (av.)	GZW volume + deglacial chronology (marine)	Bart & Tulacyzk (2020) + references therein
Palaeo-Marguerite IS	100-800	TMF volume + deglacial chronology (marine)	Dowdeswell et al. (2004)
Palaeo-Jakobshavn	1030-2300	Continental shelf basin volume + deglacial chronology (terrestrial + marine)	Hogan et al. (2012)
Palaeo-Petermann	1080-1420	GZW volume + deglacial chronology	Hogan et al. (2020)
Palaeo-Norwegian Channel IS	6000-11000	TMF volume + deglacial chronology (marine)	Nygård, 2003; Nygård et al., 2007
Subglacial Lake Whillans	< 40	Weak magnetic fabric, sediment cores; assumed ice speed, plug flow, 10 cm of deformation.	Hodson et al. (2016)
Whillans IS	~10	Extrapolation from water flux and channelised flow	Alley et al. (1989)
Whillans IS	< 88	Extrapolation from 1 × tethered stake + glaciological theory	Tulacyzk et al. (2001)
Laboratory*	0.1-1.5	Ring-shear experiments	Hansen & Zoet (2022)

Table 2: Inferred subglacial sediment fluxes under ice streams from both palaeo and modern GZ settings. Few well-constrained examples exist, and we include results from laboratory experiments (*) that aim to reproduce subglacial sediment transport to highlight the discrepancy between calculated fluxes from real and laboratory settings in addition to modern versus palaeo estimates.

The average sediment flux for the Whales Deep GZW is 1700 $m^3\ m^{-1}\ a^{-1}$, although one phase of deposition returns a flux of 4700 $m^3\ m^{-1}\ a^{-1}$ indicating that not only are the sediment fluxes in the palaeo-record much higher than modern estimates, but they may also be highly variable over time. Damsgaard et al. (2020) addressed this problem using a granular mechanical model, explaining the high palaeo-fluxes as the product of transient deepening of the "slip depth" (or shear deformation), driven by monthly-to-decadal variations in *N* (equivalent to the subglacial hydrology). Many other mechanisms have been proposed for variable slip depths in subglacial tills, based on both field work (not GZWs) and laboratory experiments (see Hansen & Zoet, 2022 for a recent discussion). However, we suggest that a promising option for understanding GZ sedimentation, and the potential for wedges to interrupt rapid GZ retreat, is to look more closely at the detailed record of sedimentation and water flow contained within the sedimentary layers of GZWs. To our knowledge no one has completed a detailed (gridded) seismic survey over a GZW, nor cored or drilled through a wedge with only surface cores having been recovered (e.g., Hanebuth et al., 2014).

5. Basal sliding and model uncertainty in grounding zones

We turn now from basal processes to how GZs are defined in models. GZs of marine ice sheets are unique problems because: (i) they have narrow geometries, which migrate; and (ii) they are subject to complex processes at their ice-bed-ocean interfaces, which evolve and, in turn, control their location. We consider each of these issues in turn.

At the scale of the ice sheet, a marine GZ represents a discontinuous transition from grounded to floating ice or, in other words, from some degree of ice-bed coupling (as determined by the basal drag term) to decoupling from the bed (zero basal drag). However, because of the discrete nature of numerical models, the traditional approach to representing a GZ is to treat it as a grounding line. This requires a transition from grounded to floating ice from one grid cell to the next and produces a discontinuous and sharp transition that is difficult to solve numerically. The grid resolution is therefore a key factor for accurately simulating GZ motion (Vieli & Payne, 2005; Leguy et al., 2014, 2021; Seroussi & Morlighem, 2018), and resolutions down to ~100 m are required for 1D Schoof-type models (Gladstone et al., 2010; Pattyn et al., 2012). However, this type of treatment has been shown to be less appropriate in cases where ice-shelf buttressing is significant (Reese et al., 2018), as is the case for many Antarctic ice streams at present. To solve such a problem, some models employ parameterisations that are able to treat the transition of basal drag within a grid cell in a continuous way should the "grounding line" lie within that cell. In other words, the basal drag term decreases smoothly to zero at the grounding line allowing for coarser resolution across the GZ (Leguy et al., 2021; Berends et al., 2025). Such ice-sheet models are often built on a model for subglacial hydrology that assumes a good connectivity between the hydrological system under grounded ice and the ocean under the ice shelf, i.e., they assume that water

pressure equals ice overburden pressure at the grounding line. In this continuous situation, resolutions of ~1 km have been shown to be sufficient when GZ connectivity to the ocean is good, or ~2 km when connectivity is low to moderate, at least for idealised model domains (Leguy et al., 2014, 2021).

As summarised by Leguy et al. (2021), several modelling techniques have been developed to address the GZ resolution issue, including grounding-line parametrisations (GLPs; e.g., Gladstone et al., 2010; Seroussi et al., 2014) and adaptive mesh refinement (AMR; Cornford et al., 2013). The former allows for sub-grid scale variations in the basal drag term proportional to the fraction of the cell that is grounded. In turn, AMR is able to increase grid resolution around the GZ domain, and in some models this increased resolution follows the GZ as it moves, maintaining higher resolution across the GZ and coarser resolution elsewhere. This prevents excessively high computational costs (Cornford et al., 2013). Still, models that employ AMR alone might still require spatial resolutions of ~1 km at the GZ, even when including higher-order stresses (Cornford et al., 2016; Cheng & Lötstedt, 2020). For this reason, ice-sheet models might seek to employ both GLPs and AMR, since they are not mutually exclusive and can be used in combination (e.g., Berends et al., 2025).

Accepting that both the model set-up and resolution at the GZ are critical for accurate model simulations (Leguy et al., 2021), we return to our second issue: the complexity of physical processes at the ice-bed-ocean boundary (Figure 1). In models, the basal sliding law chosen dictates the degree of drag at the base of the ice, so this law effectively encapsulates the variety of physical processes that contribute to the degree of coupling between the ice and its bed, i.e., the basal drag term (Table 1; Figure 1). These include (but are not limited to): deformation of subglacial sediments, ice flow over rigid obstacles (via ice deformation and sliding), and the configuration of the subglacial hydrological system including cavities and channels (see Section 4). It is standard for the current generation of models to define a basal slipperiness field, $C(x,y)$ (x and y are the horizontal Cartesian coordinates), that relates basal drag and sliding speed through the chosen sliding law. The distribution of C is then adjusted to match either present-day surface velocities (keeping the present-day ice-geometry constant), or to match the ice geometry under present-day forcings. Thus, all the physical processes that dictate basal sliding in the model are hidden in the spatial distribution of C, and their temporal evolution may not be captured (see explanation in Brondex et al., 2017).

There is an extra complexity in that each sliding law employs C differently, and often as a function of more than one variable (Table 1). In such cases, the "tuned" parameter might be one of the variables controlling C with the remaining variables kept constant. This means that different assumptions for the remaining variables can result in different values for the tuned variable. As such, even models using the same sliding law can produce different results. Nevertheless, comparisons between models and across sliding laws have shown that the resulting basal sliding coefficient C can be used interchangeably (Barnes et al., 2021). This further complicates the problem of understanding which is the best estimate for uncertain model parameters that represent processes affecting basal sliding (e.g., bed roughness, subglacial hydrology, sedimentation), as there is no unique solution to the problem.

We highlight that, for the most part, the initial basal friction field as calculated in models either does not evolve or only varies with changes in N (for sliding laws that include this dependence, Table 1). To our knowledge, there are few exceptions to this statement. In one example, a Greenland study scaled basal sliding (but not the sliding coefficients) with basal temperatures in addition to including N in the

sliding law (Cuzzone et al., 2019). Another palaeo-timescale study (last 40 Ma) modelled sediment transport under Antarctica and related basal sliding to the evolving distribution of sediments (Pollard and De Conto, 2020). For most shorter-timescale and predictive models, however, basal sliding only evolves with changes to effective pressure if this term is included in the sliding law. In other words, basal sliding as it is currently modelled, does not change due to any physical or geometrical changes at the bed involving bed roughness, bed composition, or sediment distribution. Furthermore, there are limited cases where time-evolving changes in *N* are fed back into the sliding law; so far, this has required either a fully coupled or highly simplified hydrology model (Bueler & van Pelt, 2015; Gandy et al., 2019; Pelle et al., 2024).

It is well-known that the choice of basal sliding law and its parameters is problematic for ice-sheet models due to a lack of understanding of the representative physics (Barnes et al., 2022; Hank et al., 2025). This leads to the rather circular situation described above, that the multiple bed variables that control sliding are not known and instead are tuned to match current values of ice geometry or ice velocity. Perhaps it is not surprising then that such tuned variables can return similar projections for ice loss across longer timescales (100s-1000s years): are models effectively locked into the same pattern of retreat, in terms of basal sliding, by this initial static tuning (e.g., Barnes et al., 2022; Wernecke et al., 2022)? Yet, and in contrast, multiple studies have shown that any changes to the sliding law and its variables are a significant control on retreat patterns and rates (Brondex et al., 2017, 2019; Sun et al., 2020; van der Akker et al., 2026). We suggest that this debate amongst modellers, which is illustrated by the incredibly wide spread of simulated retreat rates for both the past and future Antarctic Ice Sheet (e.g., Figure 4 in Seroussi et al., 2024), are good reasons for further consideration of basal sliding in Antarctica. We further suggest that the static basal drag term in models as they are currently set-up is a real problem, particularly across marine GZs, which are inherently characterised by multiple physical interactions between the ice, bed, and ocean that alter bed slipperiness (see Figure 1 and Section 4).

Excellent progress is being made in using measured bed properties to inform the choice of basal sliding relationships (e.g., Hank et al., 2025), and to more accurately include process variability within sliding laws (e.g., basal slip and deformation: Zoet & Iverson, 2020; transient changes in water pressure: Zoet et al., 2022; Warburton et al., 2023) and we certainly do not argue here that evolving bed information is required for all parts of the ice sheet. For example, this is not necessary for areas far inland or where ice is frozen to the bed. However, we do suggest that basal sliding laws across the GZs (plus some distance upstream) require more detailed consideration, perhaps even bespoke laws or relationships. In particular, improving representations of the spatio-temporal variability of *N*, is needed. We aim to demonstrate this requirement using our own modelling experiments in the next section.

6. Modelling grounding-zone retreat with existing sliding laws

We use the Utrecht Finite Volume Ice Sheet Model (UFEMISM; Berends et al. (2025), in this proof-of-concept work. The model domain is the entire AIS but we focus on the Weddell Sea sector and, in particular, Institute Ice Stream (IIS) as an example of an ice-stream GZ that is vulnerable to future retreat but not yet receding significantly (Siegert et al., 2016). UFEMISM employs an adaptive mesh of variable resolution, which we vary from ~2 km at the IIS GZ to ~60 km for less dynamic areas of the ice sheet (Figure S1). This ensures that we capture GZ changes accurately, especially within the IIS catchment,

which itself is simulated at resolutions < 15 km, at minimal computational expense. In addition, GZ dynamics are parameterised through a sub-grid friction scheme following Leguy et al. (2021), which bilinearly interpolates the thickness above flotation on all vertices of a given cell. The basal drag coefficient, τ_b, is then scaled by this fraction before being used in the momentum equations. Basal drag in our experiments is calculated by a sliding law that incorporates subglacial hydrology (via *N*) and combines sliding over both hard and deformable beds (Zoet & Iverson, 2020):

$$\tau_b = \min\left[N\tan(\phi), C\,u_b^{\frac{1}{m}}\right] \quad [6.1]$$

where ϕ, C, u_b and m are different parameters linked to bed conditions (see Table 1). Our experiments are initialised using a nudging procedure (Pollard & DeConto, 2012) towards the present-day Bedmap3 ice thickness (Pritchard et al., 2025); values of ϕ are iteratively adjusted until the ice sheet is in equilibrium with the forcing climate.

We then use two different parameterisations of *N* to test straightforwardly how varying subglacial hydrology (represented by *N*) affects GZ retreat. The first parameterisation follows Leguy et al. (2014), hereafter referred to as L14:

$$N = \rho_i g H \left(1 - \frac{H_f}{H}\right)^p \quad [6.2]$$

where ρ_i is the ice density, *g* is gravity, *H* the ice thickness, and $H_f = \max\left(0, -\frac{\rho_{sw}}{\rho_i} b\right)$,

with ρ_{sw} the ocean density and *b* the bed elevation (negative is below sea level). The exponent *p* therefore controls the degree of connectivity between the subglacial hydrological system and the ocean, with *p=0* resulting in no connectivity (i.e., *N* equals overburden pressure), and *p=1* is full water-pressure support from the ocean (i.e., *N=0*). In all cases where *p>0*, effective pressure is zero at the GL, ensuring a smooth transition in *N* from grounded to floating ice. In this paper, when using the L14 parameterisation we elect to use *p=1* in all cases.

The second parameterisation follows the bed elevation-scaling of Martin et al. (2011), hereafter referred to as M11:

$$N = \max(0, \rho_i g H - p_w) \quad [6.3]$$

where p_w is the porewater pressure, which linearly varies from 4% of overburden pressure at and below sea level, to full overburden pressure at and above 1000 m above sea level (a.s.l.) as in Martin et al. (2011). Such scaling with bedrock elevation is interpreted as proportional to the water content in the till, such that till is saturated at and below sea level, with its water content linearly decreasing with elevation up until 1000m a.s.l., above which ice is considered frozen to the bed.

Although both models ensure a smooth transition of basal sliding across the GZ, there are important differences in the physical reasoning between the two approaches. The L14 model with *p=1* represents a system that is well connected to the ocean, allowing full water-pressure support where ice is grounded below sea level. The degree of connectivity between the hydrological system and the ocean

is controlled by the exponent p and by how close the ice is to floatation, without any considerations regarding sediments. In M11, hydrology is assumed to depend on the ability of the till to store water. As in Martin et al. (2011), we use the elevation scaling instead of coupling porewater content to grounded-ice basal-melt rates for simplicity (c.f. Bueler and Brown, 2009). Due to the elevation-scaling in M11, the transition towards full overburden pressure inland and away from the GZ is gentler and happens over a much longer distance. Conversely, L14 reaches higher effective pressure closer to the GZ, resulting in a sharper transition from low to high effective pressure across the GZ also as it retreats inland (Figure S4).

The forcing climate has both atmospheric and oceanic components, which together yield the surface mass balance (SMB) over the entire ice sheet and the basal mass balance (BMB) under ice shelves, respectively. SMB is computed through the insolation-temperature model IMAU-ITM (Berends et al., 2018) using present-day RACMO2.3p2 temperature and precipitation (van Wessem et al., 2023) combined with present-day top-of-atmosphere insolation values (Laskar et al., 2004). The BMB is computed through a parameterisation of ice-shelf basal melting (Favier et al., 2019) that has a quadratic dependence on temperature. Ocean temperature and salinity are prescribed from a modified version of the ISMIP6 ocean temperature and salinity fields (Jourdain et al., 2020). We modify the ISMIP6 ocean forcing by cooling down the "cold" ocean cavities under the Filchner-Ronne and Ross ice shelves by 0.2 °C and 0.4°C, respectively. This is done to ensure that the GLs stay as close as possible to their Bedmap3 positions at the end of the nudging procedure, i.e., at the start of our experiments described below.

Knowing that subglacial hydrology is an important control on basal sliding, and is highly variable across marine GZs, we elect to test the ice-sheet retreat response to variations in this physical process. Previous studies have compared retreat simulations using the wide range of sliding laws available (e.g., Brondex et al., 2017, 2019; Barnes & Gudmundsson, 2022) and we do not want to simply repeat that exercise here. Rather, we use the two equations that parameterise subglacial hydrology in different ways mentioned above to see the effect on GZ retreat. We start from the equilibrium state obtained by a nudging procedure (Figure S1). This ensures that any simulated change is caused solely by the interaction between the applied forcing and our basal sliding field, which only differs because of the different parameterisations of subglacial hydrology in the sliding law. We perform four experiments, each running for 500 years and starting from the equilibrium state obtained using their respective subglacial hydrology parameterisation:

i. Unchanged climate forcing, M11hydrology parameterisation
ii. Unchanged climate forcing, L14 hydrology parameterisation
iii. Uniform 1°C increase in ocean temperature, M11 parameterisation
iv. Uniform 1°C increase in ocean temperature, L14 parameterisation

Model results. Figure 5 shows the spatial pattern of AIS retreat over the IIS region for each 500-year experiment, as well as the respective change in grounded ice area and associated sea-level rise contribution. Both models for subglacial hydrology represent the present-day GZ locations within 2 - 5 km of observations (black line in Fig. 5c) under steady state, although the L14 experiment has a better overall fit to the real GZ position for most ice streams (IS), the exception being Foundation. Similarly, both models accurately capture the ice streams in this sector with little difference in ice thickness (at time 0 years) between the M11 and L14 runs for Institute and neighbouring ice stream, Möllerisström (Fig. S5a).

When forced with 1°C of ocean warming, the loss of grounded ice during the first 50 years is similar for both M11 and L14 (Figure 5a, b), despite slight differences in GZ positions (Figures 5c, S2, S3). After 50 years, however, the experiments start to diverge substantially, with the total AIS sea-level contribution being about 1 m higher in L14 than in M11 at the end of the 500 years (Figure 5a, b). However, these changes are not uniform in their spatial or temporal patterns. The Institute GZ retreats further inland in the L14 experiment in the first 150 years, but less than in M11 after 300 years. In comparison, at 150 years the Möllerisström GZ positions for L14 and M11 are further apart than for Institute at this timestep, again with the L14 retreated farther inland, but by 300 years the furthest GZ inland is the opposite of what happened at Institute (Figure 5c). We do not explain more details about the retreat behaviours of individual ice stream catchments here because these experiments are only semi-realistic. However, it is clear that the spatial patterns and rates of retreat, as well as the timings of ice shelf pinning/unpinning are all different for experiments using the M11 or L14 hydrology models (Figures 5, S2, S3), further evidencing the sensitivity of GZ migration to how subglacial hydrology and, therefore, basal drag is prescribed across the GZ and upstream of it.

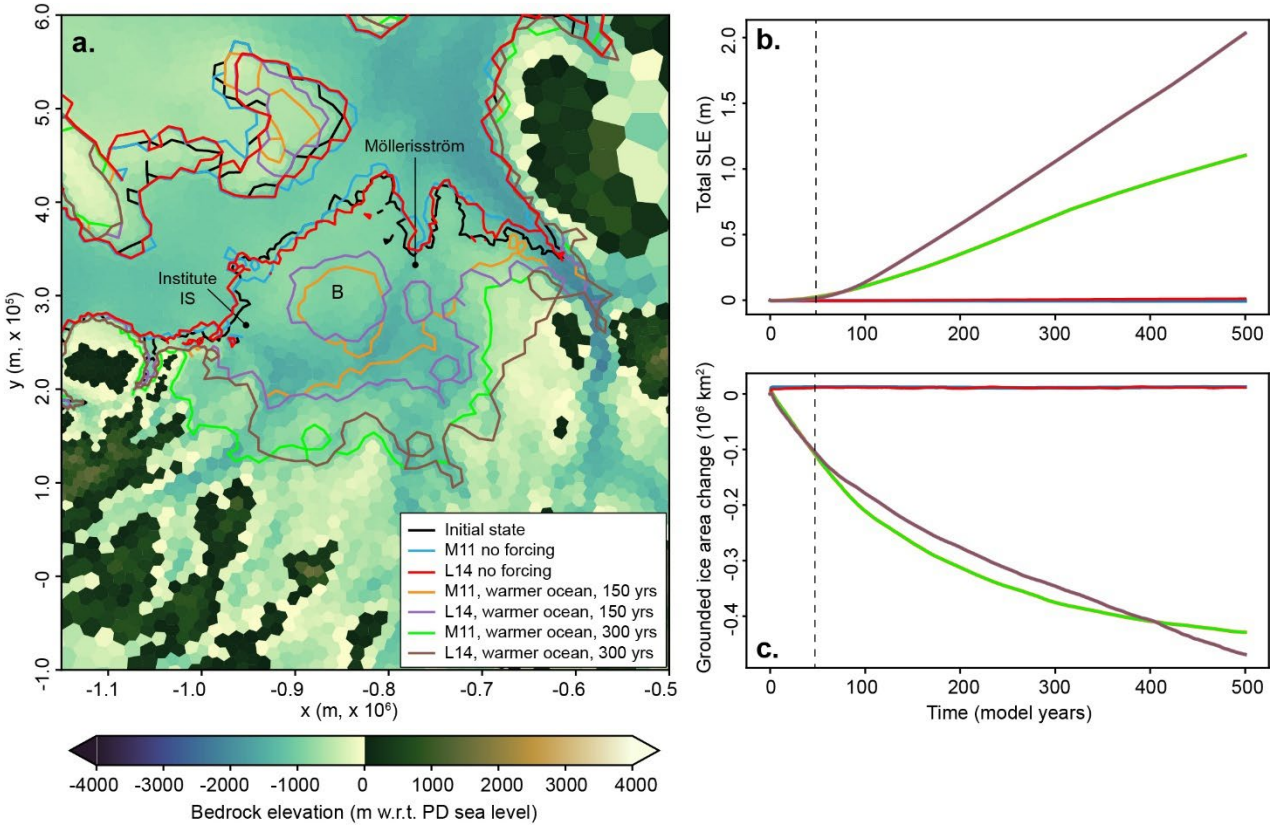

Figure 5: Evolution of GZ retreat over 500 years using different parameterisations for subglacial hydrology (via *N*). (a) Modelled GL locations at timesteps 150 and 300 years for each experiment overlain on bed topography (cells are shown in the same scale as they are represented in the model mesh; Figure S1). Coloured lines: see legend but note that black denotes the initial-condition GL and is mostly hidden by the "no forcing" runs. (b) Sea-level equivalent (SLE) during the 500-year run; (c) Change in the total area of grounded ice (negative is loss of grounded ice). Coloured lines: green is M11, brown is L14.

7. Towards improving parameterisations of GZ basal drag

Having reviewed the physical processes that occur in marine GZs (Section 4, Figure 1), it is straightforward to identify transient changes in subglacial water pressure as a key source of both spatial and temporal variability of basal drag (noting that the water pressure pushes up on the ice, the effective pressure, *N*, is the net normal stress pushing down on the bed). On the shortest timescales (hours to months), water pressure in the GZ is forced by ocean tides and potentially episodically by lake drainages. On longer timescales (years to centuries) the configuration, size and evolution of the subglacial hydrological system become important additional factors. The link between the evolving water pressure and basal drag across GZs has been clearly demonstrated by transient surface velocity changes of the ice both within and around the lateral margins of ice-stream GZs forced by ocean tides (see, for example, studies on Weddell Sea sector ice streams: Gudmundsson, 2007; Minchew et al., 2017; Rosier et al., 2017). These studies report quasi-linear decay of velocity changes as a function of distance upstream of GZ, indicating a direct link between tidal cycles and ice-stream grounding-ungrounding. Thus, there is a measurable correlation between tidal cycles and a spatial field of low-to-high basal drag that dissipates with distance away from the GZ. We suggest that such short-timescale variability, which must be added to by long-timescale change, remains a neglected component of the basal drag term in models of GZ retreat.

Accepting the above, we remember the importance of effective pressure *N* for basal sliding (see Table 1), and that *N* is related to the subglacial water pressure, w_p, via:

$$N = \rho_i g h - w_p \qquad [7.1]$$

where ρ_i is the density of the ice, g is gravity, h is the ice thickness. To focus on the subglacial hydrological system first, the range of time and length scales present in such systems has long been a modelling challenge, and one which is particularly difficult for complex ice-stream GZs. However, we know that when the ice is 100s – 1000s metres thick, as it is at Antarctic GZs, the detailed spatial and temporal evolution of basal drag is only reflected in the surface ice velocities (and hence the ice flux to the ocean) on length scales comparable to or larger than this ice thickness (Gudmundsson, 2003). This natural averaging of *N* suggests that by only using surface velocities to constrain basal sliding parameters and their coefficients, ice-sheet models are making a key simplification when upscaling their results to the length scales of the surface velocity field.

Existing models of subglacial hydrology have sought to understand the detailed evolution of the hydrological network, focussing on the evolution of Rothlisberger channels (r-channels, incised upwards into the ice) and the surrounding subglacial environment. Two examples, highlighting complementary but different approaches for the GZ are the Glacier Drainage System model (GlaDS; Werder et al., 2013) and the Subglacial Hydrology and Kinetic, Transient Interactions model (SHAKTI; Sommers et al., 2018). In GlaDS, r-channels are explicitly represented as turbulent, semi-circular channels in which melt-back and creep closure are balanced (thus maintaining the channels). The channels are represented at edges along an irregular numerical mesh and are coupled to a distributed porous subglacial environment (i.e., sediments); thus, from this network a self-organised channel system can evolve. In contrast, SHAKTI parameterises the distributed subglacial environment as thin-film flow, with r-channels included

parametrically through an evolution equation for the film thickness that, at large thicknesses, recovers a melt-creep closure balance reminiscent of r-channels. Importantly, the SHAKTI model has been incorporated into large-scale predictions of ice flow through the ISSM model (Meyer et al., 2025). Nevertheless, while both models have been used to predict the transient spatial and temporal evolution of a model subglacial hydrological system, they both rely on sufficient resolution of individual channels. Since channels can exist at an enormous range of length scales, from centimetre to 100-metre scales, this is both numerically challenging, and a significant barrier to effective comparisons with observations.

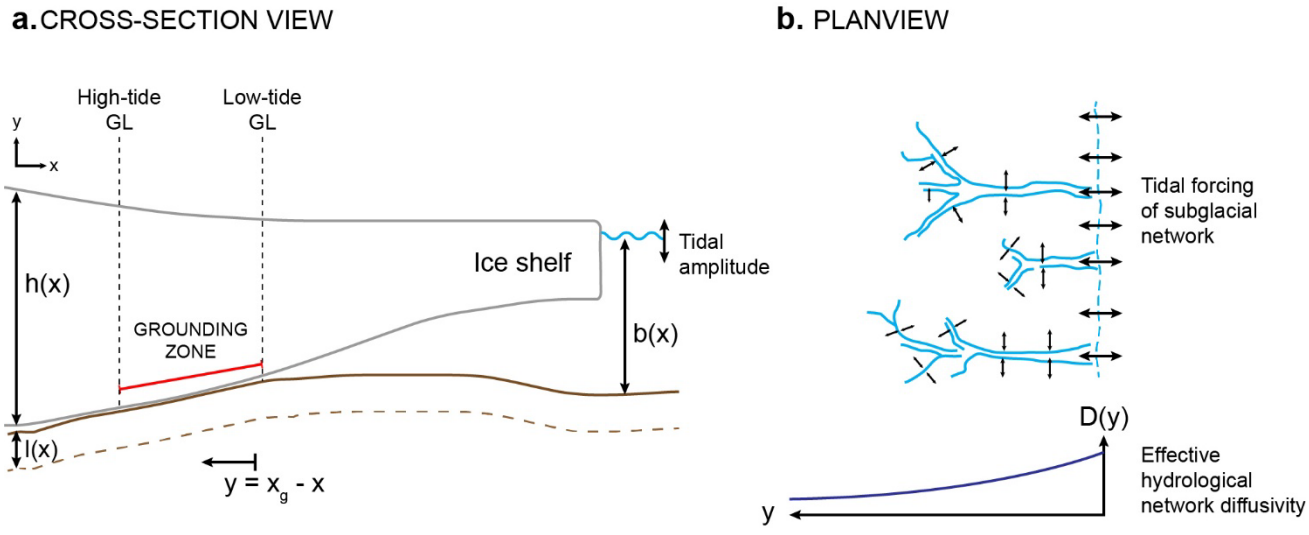

Figure 6: Schematic diagrams of an ice-stream grounding zone with tidal forcing and a channelised subglacial hydrology network in (a) cross-section and (b) planview. The elastic ice sheet lifts off the bed in the grounding zone, between the high- and low-tide grounding line (GL) positions, hence the GL migrates across the grounding zone. In (b) the effective diffusivity, *D*, is shown decreasing in magnitude away from the migrating grounding zone (dashed blue line).

Here, as in Section 6, we use subglacial hydrology as a "test case" for a relatively well-known basal process in Antarctic GZs, discussing our ideas for parameterising this process. Our approach is complementary to that of GlaDS and SHAKTI but it is predicated on the length scales over which the evolution of subglacial water pressure influences the ice flux and surface velocity field within the GZ. We treat the flow of water through the subglacial hydrological network as an effective porous Darcy flux, of the form,

$$u = -\frac{k(x,t)}{\mu}\nabla p_w, \qquad [7.2]$$

where $k(x,t)$ is the permeability of the till, μ is the viscosity of water and p_w is the water pressure. The permeability may evolve in space and time, $k = k(x,t)$, reflecting the evolution of the subglacial hydrological network. For appropriate choices of permeability, this formalism either recovers porous flow through till or the flux of water through thin films and cavities in the subglacial environment. Hence, over

the depth $l(x)$ the hydraulically active portion of the subglacial environment the water pressure is determined by,

$$S\frac{\partial p_w}{\partial t} + \nabla \cdot (lu) = 0, \qquad [7.3]$$

where here S is the specific storativity (of a system in groundwater hydrology; Pinder & Celia, 2006) and relates the storage of water to the pressure field (through compressibility of water, the matrix or storage in the englacial system). It is worth noting that for small values of storativity, the system recovers the elliptic nature of the system characteristically solved in SHAKTI and can be made equivalent for a suitable choice of the permeability.

As a simple, representative example, we calculate the water pressure as a function of distance x inland of the GZ (Figure 6). We take $x = 0$ as the seaward limit. At this limit $p_w(x,t)$, can be illustrated for the tidal forcing of a uniform subglacial system (assuming constant and uniform permeability and storativity). In such a case, the pressure obeys a simplified diffusion equation,

$$\frac{\partial p_w}{\partial t} = \frac{\partial}{\partial x}\left(D\frac{\partial p_w}{\partial x}\right), \qquad [7.4]$$

where $D = lk / \mu S$ is the effective diffusivity of pressure. While complex in detail, the tidal forcing may be represented as an oscillatory forcing at $x = 0$ of the form

$$p_w(0,t) = \rho_w g\left[\overline{b}(0) + \Delta b\cos(\omega t)\right], \qquad [7.5]$$

for the effective tidal forcing frequency ω. Here, the mean pressure (averaged over the tidal cycle) is taken to be the hydrostatic pressure $\rho_w g\overline{b}(0)$ at $x = 0$, written here in terms of the water depth $b(x)$ which tidally varies about the mean, $b(0,t) = \overline{b}(0) + \Delta b\cos(\omega t)$. Solutions for the subglacial water pressure inland are therefore given by

$$p_w(x,t) = \rho_w g\left[\overline{b}(0) + \Delta b\, e^{-\sqrt{\frac{\omega}{2D}}x}\cos\left(\omega t - \sqrt{\frac{\omega}{2D}}x\right)\right]. \qquad [7.6]$$

As an exemplar of a pipeline between a GZ basal process (here, tides) and variable basal drag, this model of water pressure across the GZ may be related to the effective pressure, *N*, which in turn can be related to variations in the surface speed of the ice. For example, the surface ice velocity may be related to the extensional stresses in the ice, the basal drag, and the driving gravitational stress (respectively in the equation below), through a vertically-integrated stress balance (Schoof, 2007; Tsai et al., 2015),

$$2A^{-1/n}\left(hu_x^{1/n}\right)_x - \tau_b - \rho g\left(h - \overline{b}\right)x = 0, \qquad [7.7]$$

where u is the velocity of the ice, A and n are the rate factor and exponent in Glen's flow law, h is the ice thickness and $\overline{b}(x)$ is the depth of the seafloor (we neglect tidal variations in the force balance), ρ is the density of ice, g is the gravitational acceleration and τ_b is basal drag (discussed earlier). Thus, for example, using a Coulomb model for the basal drag (See Table 1; Iverson et al, 1998), basal drag is given by

$$\tau_b = \mu(p_i - p_w) = \overline{\tau_b} + \Delta\tau_b, \qquad [7.8]$$

and can be decomposed into mean ($\overline{\tau_b}$) and time varying ($\Delta\tau_b$) components so that

$$\overline{\tau_b(x)} = \mu\rho g\left[h - \frac{\rho_w}{\rho}\overline{b}(0)\right] \text{ and } \Delta\tau_b(x,t) = \mu\rho_w g \Delta b e^{-\sqrt{\frac{\omega}{2D}}x}\cos\left(\omega t - \sqrt{\frac{\omega}{2D}}x\right), \qquad [7.9]$$

where typically $\Delta\tau_b \ll \overline{\tau_b}$. Hence, the velocity response can likewise be decomposed into a mean and time varying component, $u = \overline{u(x)} + \Delta u(x,t)$, in which $\Delta u \ll \overline{u}$. A linearisation of the stress balance in the ice for small variations in basal drag therefore gives

$$\frac{2A^{-1/n}}{n}\left[h\left(\Delta u\,\overline{u}^{\frac{1}{n}-1}\right)_x\right]_x = \Delta\tau_b. \qquad [7.10]$$

The temporal variation of the basal drag is mirrored in the surface velocity field, with the spatial variation (in distance x from the grounding line) influenced by the profiles of the background ice thickness and velocity fields ($h, \overline{u}$). This suggests that measurements of the surface velocity variations on short timescales (hours to weeks) can be used to infer the subglacial environment (i.e., the bed characteristics), and that longer-term variations in the velocity fluctuations of the ice (seasonal to decadal timescales) might be used to infer the evolution of the subglacial hydrological network.

Time-varying basal drag over soft, deformable sediments will also produce a time-varying rate of sediment transport across the GZ (see Section 4 for a real-life example from Whales Deep, Ross Sea). Sediment mobillisation is likely to be highly sensitive to the porewater pressure (and hence effective pressure N), and the power-law rheology has previously approximated this with a yield stress ~100kPa (Tsai et al., 2015; Zoet & Iverson, 2020). Hence, variations of N on short (tidal) or longer (seasonal or inter-annual) timescales is likely to lead to variations in the sediment flux which act to evolve and change the bed geometry across the GZ. It is also worth noting that while surface velocity variations may be used to infer variations in N on the scale of the ice-sheet thickness, such variations in N are likely to also be highly spatially variable, with significant differences between any incipient channel network and the surrounding bed of either till or rough bedrock. This means that small-scale models that can facilitate interpretation of the configuration of the subglacial hydrological network from larger-scale remote measurements (e.g., satellites) are a potentially important tool to characterise the spatial and temporal redistribution of subglacial sediments in the GZ, and the effect on ice flow. Previous studies have alluded to this by linking the findings from small-scale mathematical models to field observations at Antarctic

GZs (e.g., for tidal migration Warburton et al., 2020) but here we argue that such models could provide the stepping stone between complex field observations and ice-sheet model parameterisations.

8. Discussion

The Antarctic Ice Sheet remains the largest source of uncertainty in sea-level projections. Modelling its ice loss to 2300 returns an extremely wide range of values, equivalent to a 0.3 m drop in global sea level to a 6.9 m SLE (ISMIP6 forcing, high emission scenario with ice-shelf collapse; Seroussi et al., 2024). This spread underlines the dominant question for our community: **how can we reduce uncertainty in Antarctic ice loss and sea-level rise projections?**

For the past ~20 years the idea that ocean-driven melting of ice shelves causes them to thin and lose buttressing strength, resulting in acceleration of ice streams flowing into them, has been a cornerstone of Antarctic glaciology. *In extremis*, the loss of entire ice shelves is predicted to "uncork" the upstream grounded ice sheet and potentially lead to runaway decay as ice streams discharge into the surrounding ocean (Pritchard et al., 2012; Gudmundsson et al., 2019). Accurate projections of this decay require robust representations of GZ dynamics (Schoof, 2007; Brondex et al., 2019) as these ice-sheet edge locations will determine the size and shape of the AIS as it retreats. Returning to the force balance for GZs (Figure 1), we must acknowledge that ice-shelf melting (loss of buttressing) is only part of the story for locating GZs when we think about the forces that oppose gravitational driving stress. In comparison with the loss of ice-shelf side drag, the basal drag term has remained under-studied despite acceptance that: (i) basal drag has a strong influence on ice dynamics (Schoof, 2007; Tsai et al., 2015); (ii) the choice of basal sliding law exerts a strong control on retreat simulations (Ritz et al., 2015; Brondex et al., 2017, 2019); (iii) there is a need to include more basal processes constrained by observations in sliding laws (Koellner et al., 2019; Hager et al., 2022; Kazmierczak et al., 2024). These statements become acute at ice-stream GZs because they dictate the ice flux to the ocean, and because GZs are inherently characterised by a complex and variable basal drag field (see Section 4).

To make the case for renewed focus on Antarctic GZ basal drag, we point out that all ISMIP6 models in Seroussi et al. (2024) resolve widespread ice-shelf collapse from ~2150 (high-emissions scenario). After collapse, ice-shelf melting presumably diminishes in its influence on the GZ force balance whereas basal drag would rise in significance, as is interpreted to happen at the Whales Deep GZW for a period of ~1000 years (Bart et al., 2017), or as has been observed recently at TG after the loss of buttressing strength of the Thwaites Glacier Tongue (Parizek et al., 2013). Indeed, recent model results suggest that ice-shelf melting will have a limited influence on the retreat of TG going forwards (Gudmundsson et al., 2023; Bett et al., 2024; Williams et al., *in review*). For the period up to collapse, even if researchers achieve a perfect melt parameterisation – indeed, there are numerous groups working on this and performing bespoke comparisons studies (e.g., Favier et al., 2019; Burgard et al., 2022) - we assert that we cannot yet model retreat robustly because the basal drag term does not account for the true variability across GZs. We attempted to evidence this assertion in our model runs in Section 6 by only varying the hydrology-related term of the basal sliding law and returning variable patterns of GZ retreat (Figure 5). However, to fully quantify the relative importance of different basal drag parametrisations (i.e., basal sliding laws and coefficients) versus melt parameterisations, on GZ retreat would require the same model initialisation process, the same set-up for the grounding line, and to use

the same basal sliding laws and melt parameterisations, only varying the latter independently. To our knowledge, this type of experiment has not been performed for forward projections extending over centuries, which means that when uncertainty attribution studies are carried out in AIS projections, basal sliding is usually not assessed despite being recognised as a major source of uncertainty (e.g., Bulthuis et al., 2019; Coulon et al., 2024). Gladstone et al. (2017) probably came closest when they compared parameterisations for basal sliding and ice-shelf melting in flow-line retreat simulations, although their goal was to determine the model resolution required at the GL not to assess which parameterisation had the biggest effect on retreat.

Furthermore, there is a fundamental difference between the melt parameterisations and the basal sliding parameterisations used in models forecasting AIS mass loss: melt rates will vary with time according to the changing ocean forcing and as water depths vary in evolving ice-shelf cavities. In contrast, as we describe in Section 5, the basal drag field remains largely static (or only varies with *N*) over time. We see this discrepancy as a fundamental limitation to our ability to model Antarctic GZs and would argue that this places more uncertainty in the basal drag term than in the ice-shelf melt/buttressing term. In Section 7, we explored how mathematical process models might be used to accommodate a range of GZ basal processes in our basal sliding laws (or a series of relationships?) whilst also allowing for each process to evolve over time and space. If we imagine applying a set of bespoke sliding laws at the GZ plus some distance upstream, say 10 km, then when the GZ retreated the 10-km GZ sliding laws would also move inland tracking the ice-sheet edge backwards. Conforming with how existing sliding laws are taken up in ice-sheet models would be an important requirement for this process so that any new sliding relationships could be "plugged-in" to existing models.

In this paper, we have discussed the high variability of GZ basal drag primarily in relation to two physical processes: subglacial hydrology and sedimentation. This is because: (i) far more progress has been made around understanding and modelling subglacial hydrology than many other basal processes in GZs; and (ii) sediment wedge-building is the fastest known negative feedback on ice-sheet retreat, yet it is understudied and not included in ice-sheet models in any way. There are now multiple examples of sediments providing stabilisation at present-day ice-stream GZs, either by actively building topography or by increasing basal drag as sediment properties change (Horgan et al., 2013, 2021; Walker et al., 2013; Siegert et al., 2016). Even a cursory examination of data over several ice-stream beds from their GZs inland (see Supplementary Figures S6-S13) provides an exciting discovery in what appears to be a GZW at the eastern end of the Institute Ice Stream GZ (Figure S9). We discussed some of the challenges to incorporating wedge-building into ice-sheet models in Section 4.5, namely a lack of understanding of the mechanisms of: (i) subglacial sediment transport and (ii) the exceptionally high palaeo-sediment fluxes. Wedge-building is clearly an episodic process but one that could counter the highest ice-shelf melt rates reported from GZs (melt rates: 10s of m a^{-1} versus sediment fluxes from GZWs: 1000s-10000s m^3 m^{-1} a^{-1}). Although wedge-building essentially generates a new pinning point at a GZ (by raising the bed elevation) we acknowledge the strong link to basal drag via the deposition of "sticky" till units or altering the bed roughness at small scales (~10s metres), or some combination thereof. Thus, we would propose to incorporate wedge-building into our series of GZ sliding relationships, altering the basal drag in relation to the evolving distribution of sediments and roughness but also allowing the bed topography to change. Additional processes that change the bed geometry, such as GIA or bed erosion by water or ice, could be

incorporated into such sliding relationships, thus providing an efficient way to include dynamic topography at Antarctic GZs into models without requiring full coupling to computationally-heavy sediment erosion/transport models.

9. Future directions

We can summarise this work by identifying four major limitations to improving our understanding of basal drag in Antarctic GZs:

i. Lack of observations of basal properties at the spatial and temporal scales important for ice flow;
ii. Lack of understanding of the critical scales of basal processes: fine-scale processes are challenging to observe yet may be critical for ice dynamics;
iii. Absence of time-evolving basal processes in basal sliding laws;
iv. Absence of bed evolution and sedimentation in ice-sheet models.

In Section 6 we provided an exemplar for how temporally- and spatially-varying bed characteristics could be incorporated into basal sliding laws via mathematical process models. However, it is clear from (i) and (ii) above and from the discussion throughout Section 4, that such relationships need to be constrained by observations despite the challenging nature of working at Antarctic GZs (Parizek, 2024; Fricker et al., 2025). Without exception, theoretical modelling studies conclude that the behaviour of ice across a given GZ will depend on local basal conditions (e.g., Walker et al., 2013; Robel et al., 2022). Thus, any models attempting to allow basal drag to evolve must not only capture the relevant temporal scales for ice-sheet change - from hours to many years - but they must also adequately cover the range of GZ bed types and ice dynamics.

We suggest that what is needed is a careful selection of observations from workable GZs that exhibit a range of dynamic ice behaviours. For example, Freer et al. (2023) used repeat satellite altimetry to identify four different types of ice-dynamic response to the same tidal forcing at the GZ of Bungenstock Ice Rise and this work could be extended to other GZ locations, alongside an analysis of GZ geometry types (e.g., Supp. Figures S6-S13) to identify spatial variability in both GZ ice behaviour and bed composition. Such efforts could be maximised by concomitant exploration of the full GZ process parameter space using inexpensive models in a two-way set up where models could guide the strategy for field observations, as well as then using field observations to constrain the model experiments. Unfortunately, we cannot measure effective pressure directly, nor can we measure subglacial water pressure on scales that are useful for models (note the ~5 km mesh size of UFEMISM at the GZ in our experiments), although point bed measurements of water pressure are possible (e.g., using Cryoegg probes; Prior-Jones et al., 2025). We are, however, now able to measure things like bed morphology in 3D using the relatively new swath-radar capability (Holschuh et al., 2021) or subsurface bed type (soft, hard, mixed) in near-3D and on repeat using a combination of efficient seismic drag-cable systems, repeat radar surveys, and EM stations. Such holistic studies of ice-streams GZs (e.g., Agnew et al., 2026) are essential if we are to understand the nature of bed coupling/uncoupling in this critical zone. If a GZ was instrumented over a series of weeks for several Antarctic field seasons this could return ~4 weeks of measurements across 2-3 years, thus covering the full range of tidal variability and year-on-year changes. One challenge is to link observations of bed conditions that can be made over hours to ~weeks in this

way, to bed changes in the GZ on the longer timescales that affect ice dynamics (i.e., multidecadal to centennial). We suggest that detailed geophysical observations over GZWs may provide the only record of GZ change across long-timescales because the wedges are known to preserve evidence of sedimentation, fluid flow, subglacial channels, and bed morphology within their sedimentary sequences which build up over decades to centuries.

We recognise that this study is by no means a full review of basal sliding, ice-sheet models or GZ basal processes including sedimentation. Rather, our aim was to build bridges between the different communities trying to help understand the very edges of the AIS, be they remote sensors, glaciologists and palaeo-glaciologists, or numerical modellers. The rate of progress in the field of ice-ocean interactions, be that in ice-sheet model design or in the genesis and implementation of ice-shelf melt parameterisations, is impressive. Commensurate focused work on GZ basal sliding can improve understanding of ice behaviour at the critical ice-ocean boundary and allow us to narrow the uncertainty in our projections of AIS decay and sea-level rise. The growing desire for multidisciplinary work and the use of inexpensive mathematical models as a pipeline from field or laboratory studies to ice-sheet models should enable rapid progress.

Acknowledgements: This work is supported by the Polar Science for a Sustainable Planet programme at the British Antarctic Survey (KAH, AMB, CM, MMB, OM, RL); KW was supported by a Junior Research Fellowship, Trinity College, University of Cambridge. BK acknowledges his NERC-IGIS grant (NE/R010838/1) which provided some motivation for this work. We would like to thank Keith Nicholls, Robert Arthern, James Smith, and Kevin Hank for helpful discussions about the ideas put forward in this paper.

References:

Adhikari, S., & J. Marshall, S. (2012). Parameterization of lateral drag in flowline models of glacier dynamics. Journal of Glaciology, 58(212), 1119-1132. https://doi.org/10.3189/2012JoG12J018

Agnew, R. S., Pearce, E., Karplus, M., Ranganathan, M., Hoffman, A. O., Hunt, M., Pretorius, A., Shanly, S. E., Beres, M., Pradhan, K. K., Seldon, Y., Booth, A. D., Clark, R. A., & Jan Young, T. (2025). Active and Passive Seismic Surveys over the Grounding Zone of Eastwind Glacier, Antarctica. Seismological Research Letters, 97(1), 591-605. https://doi.org/10.1785/0220250024

Aitken, A. R. A., Li, L., Kulessa, B., Schroeder, D., Jordan, T. A., Whittaker, J. M., Anandakrishnan, S., Dawson, E. J., Wiens, D. A., Eisen, O., & Siegert, M. J. (2023). Antarctic Sedimentary Basins and Their Influence on Ice-Sheet Dynamics. Reviews of Geophysics, 61(3), e2021RG000767. https://doi.org/https://doi.org/10.1029/2021RG000767

Åkesson, H., Morlighem, M., O'Regan, M., & Jakobsson, M. (2021). Future Projections of Petermann Glacier Under Ocean Warming Depend Strongly on Friction Law. Journal of Geophysical Research: Earth Surface, 126(6), e2020JF005921. https://doi.org/https://doi.org/10.1029/2020JF005921

Alley, K. E., Scambos, T. A., Siegfried, M. R., & Fricker, H. A. (2016). Impacts of warm water on Antarctic ice shelf stability through basal channel formation. Nature Geoscience, 9(4), 290-293. https://doi.org/10.1038/ngeo2675

Alley, R. B., Anandakrishnan, S., Dupont, T. K., Parizek, B. R., & Pollard, D. (2007). Effect of Sedimentation on Ice-Sheet Grounding-Line Stability. Science, 315(5820), 1838-1841. https://doi.org/10.1126/science.1138396

Alley, R., Blankenship, D., Bentley, C. & Rooney, & S. T. (1986). Deformation of till beneath ice stream B, West Antarctica. Nature, 322, 57–59. https://doi.org/10.1038/322057a0

Alley, R. B., Blankenship, D. D., Bentley, C. R. & Rooney, S. T. (1987). Till beneath ice stream B: 3. Till deformation: Evidence and implications, Journal of Geophysical Research, 92(B9), 8921–8929, doi:10.1029/JB092iB09p08921

Alley, R., Blankenship, D., Bentley, C. & Rooney, & S. T. (1989). Sedimentation beneath ice shelves — the view from ice stream B. Marine Geology, 85 (2-4). https://doi.org/10.1016/0025-3227(89)90150-3

Alley, R. B., Holschuh, N., MacAyeal, D. R., Parizek, B. R., Zoet, L., Riverman, K., Muto, A., Christianson, K., Clyne, E., Anandakrishnan, S., Stevens, N., & Collaboration, G. (2021). Bedforms of Thwaites Glacier, West Antarctica: Character and Origin. Journal of Geophysical Research: Earth Surface, 126(12), e2021JF006339. https://doi.org/https://doi.org/10.1029/2021JF006339

Anandakrishnan, S., Catania, G. A., Alley, R. B., & Horgan, H. J. (2007). Discovery of Till Deposition at the Grounding Line of Whillans Ice Stream. Science, 315(5820), 1835-1838. https://doi.org/10.1126/science.1138393

Arthern, R. J., Hindmarsh, R. C. A., & Williams, C. R. (2015). Flow speed within the Antarctic ice sheet and its controls inferred from satellite observations. Journal of Geophysical Research: Earth Surface, 120(7), 1171-1188. https://doi.org/https://doi.org/10.1002/2014JF003239

Barletta, V. R., Bevis, M., Smith, B. E., Wilson, T., Brown, A., Bordoni, A., Willis, M., Khan, S. A., Rovira-Navarro, M., Dalziel, I., Smalley, R., Kendrick, E., Konfal, S., Caccamise, D. J., Aster, R. C., Nyblade, A., & Wiens, D. A. (2018). Observed rapid bedrock uplift in Amundsen Sea Embayment promotes ice-sheet stability. Science, 360(6395), 1335-1339. https://doi.org/10.1126/science.aao1447

Barnes, J. M., & Gudmundsson, G. H. (2022). The predictive power of ice sheet models and the regional sensitivity of ice loss to basal sliding parameterisations: a case study of Pine Island and Thwaites glaciers, West Antarctica. The Cryosphere, 16(10), 4291-4304. https://doi.org/10.5194/tc-16-4291-2022

Bart, P. J., & Cone, A. N. (2012). Early stall of West Antarctic Ice Sheet advance on the eastern Ross Sea middle shelf followed by retreat at 27,50014CyrBP. Palaeogeography, Palaeoclimatology, Palaeoecology, 335-336, 52-60. https://doi.org/https://doi.org/10.1016/j.palaeo.2011.08.007

Bart, P. J., DeCesare, M., Rosenheim, B. E., Majewski, W., & McGlannan, A. (2018). A centuries-long delay between a paleo-ice-shelf collapse and grounding-line retreat in the Whales Deep Basin, eastern Ross Sea, Antarctica. Scientific Reports, 8(1), 12392. https://doi.org/10.1038/s41598-018-29911-8

Bart, P. J., Krogmeier, B. J., Bart, M. P., & Tulaczyk, S. (2017). The paradox of a long grounding during West Antarctic Ice Sheet retreat in Ross Sea. Scientific Reports, 7(1), 1262. https://doi.org/10.1038/s41598-017-01329-8

Bart, P. J., & Owolana, B. (2012). On the duration of West Antarctic Ice Sheet grounding events in Ross Sea during the Quaternary. Quaternary Science Reviews, 47, 101-115. https://doi.org/https://doi.org/10.1016/j.quascirev.2012.04.023

Bart, P. J., & Tulaczyk, S. (2020). A significant acceleration of ice volume discharge preceded a major retreat of a West Antarctic paleo–ice stream. Geology, 48(4), 313-317. https://doi.org/10.1130/G46916.1

Batchelor, C. L., & Dowdeswell, J. A. (2015). Ice-sheet grounding-zone wedges (GZWs) on high-latitude continental margins. Marine Geology, 363, 65-92. https://doi.org/https://doi.org/10.1016/j.margeo.2015.02.001

Berends, C. J., Azizi, V., Bernales, J. A., & van de Wal, R. S. W. (2025). The Utrecht Finite Volume Ice-Sheet Model (UFEMISM) version 2.0 – Part 1: Description and idealised experiments. Geosci. Model Dev., 18(12), 3635-3659. https://doi.org/10.5194/gmd-18-3635-2025

Berends, C. J., de Boer, B., & van de Wal, R. S. W. (2018). Application of HadCM3@Bristolv1.0 simulations of paleoclimate as forcing for an ice-sheet model, ANICE2.1: set-up and benchmark experiments. Geosci. Model Dev., 11(11), 4657-4675. https://doi.org/10.5194/gmd-11-4657-2018

Bett, D. T., Bradley, A. T., Williams, C. R., Holland, P. R., Arthern, R. J., & Goldberg, D. N. (2024). Coupled ice–ocean interactions during future retreat of West Antarctic ice streams in the Amundsen Sea sector. The Cryosphere, 18(6), 2653-2675. https://doi.org/10.5194/tc-18-2653-2024

Bjarnadóttir, L. R., Rüther, D. C., Winsborrow, M. C. M., & Andreassen, K. (2013). Grounding-line dynamics during the last deglaciation of Kveithola, W Barents Sea, as revealed by seabed geomorphology and shallow seismic stratigraphy. Boreas, 42(1), 84-107. https://doi.org/https://doi.org/10.1111/j.1502-3885.2012.00273.x

Blankenship, D. D., Rooney, S. T., Alley, R. B., & Bentley, C. R. (1989). Seismic Evidence for a Thin Basal Layer at a Second Location on Ice Stream B, Antarctica. Annals of Glaciology, 12, 200-200. https://doi.org/10.3189/S0260305500007217

Book, C., Hoffman, M. J., Kachuck, S. B., Hillebrand, T. R., Price, S. F., Perego, M., & Bassis, J. N. (2022). Stabilizing effect of bedrock uplift on retreat of Thwaites Glacier, Antarctica, at centennial

timescales. Earth and Planetary Science Letters, 597, 117798. https://doi.org/https://doi.org/10.1016/j.epsl.2022.117798

Bradley, A. T., & Hewitt, I. J. (2024). Tipping point in ice-sheet grounding-zone melting due to ocean water intrusion. Nature Geoscience, 17(7), 631-637. https://doi.org/10.1038/s41561-024-01465-7

Brondex, J., Gagliardini, O., Gillet-Chaulet, F., & Durand, G. (2017). Sensitivity of grounding line dynamics to the choice of the friction law. Journal of Glaciology, 63(241), 854-866. https://doi.org/10.1017/jog.2017.51

Brondex, J., Gillet-Chaulet, F., & Gagliardini, O. (2019). Sensitivity of centennial mass loss projections of the Amundsen basin to the friction law. The Cryosphere, 13(1), 177-195. https://doi.org/10.5194/tc-13-177-2019

Brunt, K. M., Fricker, H. A., & Padman, L. (2011). Analysis of ice plains of the Filchner–Ronne Ice Shelf, Antarctica, using ICESat laser altimetry. Journal of Glaciology, 57(205), 965-975. https://doi.org/10.3189/002214311798043753

Budd, W. F., Keage, P. L., & Blundy, N. A. (1979). Empirical Studies of Ice Sliding. Journal of Glaciology, 23(89), 157-170. https://doi.org/10.3189/S0022143000029804

Bueler, E., & Brown, J. (2009). Shallow shelf approximation as a "sliding law" in a thermomechanically coupled ice sheet model. Journal of Geophysical Research: Earth Surface, 114(F3). https://doi.org/https://doi.org/10.1029/2008JF001179

Bueler, E., & van Pelt, W. (2015). Mass-conserving subglacial hydrology in the Parallel Ice Sheet Model version 0.6. Geosci. Model Dev., 8(6), 1613-1635. https://doi.org/10.5194/gmd-8-1613-2015

Bulthuis, K., Arnst, M., Sun, S., & Pattyn, F. (2019). Uncertainty quantification of the multi-centennial response of the Antarctic ice sheet to climate change. The Cryosphere, 13(4), 1349-1380. https://doi.org/10.5194/tc-13-1349-2019

Burgard, C., Jourdain, N. C., Reese, R., Jenkins, A., & Mathiot, P. (2022). An assessment of basal melt parameterisations for Antarctic ice shelves. The Cryosphere, 16(12), 4931-4975. https://doi.org/10.5194/tc-16-4931-2022

Cairns, G. J., Benham, G. P., & Hewitt, I. J. (2025). Groundwater dynamics beneath a marine ice sheet. The Cryosphere, 19(9), 3725-3747. https://doi.org/10.5194/tc-19-3725-2025

Calkin, T., Dunbar, G. B., Atkins, C., Carter, A., Coenen, J. J., Eaves, S., Ginnane, C. E., Golledge, N. R., Harwood, D. M., Horgan, H. J., Hurwitz, B. C., Hulbe, C., Lawrence, J. D., Levy, R., Marschalek, J. W., Martin, A. P., Mullen, A. D., Neuhaus, S., Quartini, E., . . . Washam, P. M. (2024). Recent sedimentology at the grounding zone of the Kamb Ice stream, West Antarctica and implications for ice shelf extent. Quaternary Science Reviews, 344, 108988. https://doi.org/https://doi.org/10.1016/j.quascirev.2024.108988

Carter, S. P., & Fricker, H. A. (2012). The supply of subglacial meltwater to the grounding line of the Siple Coast, West Antarctica. Annals of Glaciology, 53(60), 267-280. https://doi.org/10.3189/2012AoG60A119

Chen, H., Rignot, E., Scheuchl, B., & Ehrenfeucht, S. (2023). Grounding Zone of Amery Ice Shelf, Antarctica, From Differential Synthetic-Aperture Radar Interferometry. Geophysical Research Letters, 50(6), e2022GL102430. https://doi.org/https://doi.org/10.1029/2022GL102430

Cheng, C., Jenkins, A., Holland, P. R., Wang, Z., Dong, J., & Liu, C. (2024). Ice shelf basal channel shape determines channelized ice-ocean interactions. Nature Communications, 15(1), 2877. https://doi.org/10.1038/s41467-024-47351-z

Christian, J. E., Robel, A. A., Catania, G. A., Stearns, L. A., Miller, L. E., & Garcia, S. M. (2024). Grounding-Zone Wedge Formation and Effects on Ice-Stream Retreat and Stability. Authorea Preprints.

Christianson, K., Jacobel, R. W., Horgan, H. J., Alley, R. B., Anandakrishnan, S., Holland, D. M., & DallaSanta, K. J. (2016). Basal conditions at the grounding zone of Whillans Ice Stream, West Antarctica, from ice-penetrating radar. Journal of Geophysical Research: Earth Surface, 121(11), 1954-1983. https://doi.org/https://doi.org/10.1002/2015JF003806

Christianson, K., Parizek, B. R., Alley, R. B., Horgan, H. J., Jacobel, R. W., Anandakrishnan, S., Keisling, B. A., Craig, B. D., & Muto, A. (2013). Ice sheet grounding zone stabilization due to till compaction. Geophysical Research Letters, 40(20), 5406-5411. https://doi.org/https://doi.org/10.1002/2013GL057447

Christie, F. D. W., Bingham, R. G., Gourmelen, N., Tett, S. F. B., & Muto, A. (2016). Four-decade record of pervasive grounding line retreat along the Bellingshausen margin of West Antarctica. Geophysical Research Letters, 43(11), 5741-5749. https://doi.org/https://doi.org/10.1002/2016GL068972

Clarke, G. K. C. (2005). SUBGLACIAL PROCESSES. Annual Review of Earth and Planetary Sciences, 33(Volume 33, 2005), 247-276. https://doi.org/https://doi.org/10.1146/annurev.earth.33.092203.122621

Cornford, S. L., Martin, D. F., Graves, D. T., Ranken, D. F., Le Brocq, A. M., Gladstone, R. M., Payne, A. J., Ng, E. G., & Lipscomb, W. H. (2013). Adaptive mesh, finite volume modeling of marine ice sheets. Journal of Computational Physics, 232(1), 529-549. https://doi.org/https://doi.org/10.1016/j.jcp.2012.08.037

Coulon, V., Klose, A. K., Kittel, C., Edwards, T., Turner, F., Winkelmann, R., & Pattyn, F. (2024). Disentangling the drivers of future Antarctic ice loss with a historically calibrated ice-sheet model. The Cryosphere, 18(2), 653-681. https://doi.org/10.5194/tc-18-653-2024

Cuzzone, J. K., Schlegel, N. J., Morlighem, M., Larour, E., Briner, J. P., Seroussi, H., & Caron, L. (2019). The impact of model resolution on the simulated Holocene retreat of the southwestern Greenland ice sheet using the Ice Sheet System Model (ISSM). The Cryosphere, 13(3), 879-893. https://doi.org/10.5194/tc-13-879-2019

Damsgaard, A., Goren, L., & Suckale, J. (2020). Water pressure fluctuations control variability in sediment flux and slip dynamics beneath glaciers and ice streams. Communications Earth & Environment, 1(1), 66. https://doi.org/10.1038/s43247-020-00074-7

De Rydt, J., & Naughten, K. (2024). Geometric amplification and suppression of ice-shelf basal melt in West Antarctica. The Cryosphere, 18(4), 1863-1888. https://doi.org/10.5194/tc-18-1863-2024

Doake, C. S. M. (1978). Dissipation of tidal energy by Antarctic ice shelves. Nature, 275(5678), 304-305. https://doi.org/10.1038/275304a0

Dorschel, B., Hehemann, L., Viquerat, S., Warnke, F., Dreutter, S., Tenberge, Y. S., Accettella, D., An, L., Barrios, F., Bazhenova, E., Black, J., Bohoyo, F., Davey, C., De Santis, L., Dotti, C. E., Fremand, A. C., Fretwell, P. T., Gales, J. A., Gao, J., . . . Arndt, J. E. (2022). The International Bathymetric Chart of the Southern Ocean Version 2. Scientific Data, 9(1), 275. https://doi.org/10.1038/s41597-022-01366-7

Dow, C. F., Ross, N., Jeofry, H., Siu, K., & Siegert, M. J. (2022). Antarctic basal environment shaped by high-pressure flow through a subglacial river system. Nature Geoscience, 15(11), 892-898. https://doi.org/10.1038/s41561-022-01059-1

Dowdeswell, J. A., & Fugelli, E. M. G. (2012). The seismic architecture and geometry of grounding-zone wedges formed at the marine margins of past ice sheets. GSA Bulletin, 124(11-12), 1750-1761. https://doi.org/10.1130/B30628.1

Dowdeswell, J. A., Hogan, K. A., Arnold, N. S., Mugford, R. I., Wells, M., Hirst, J. P. P., & Decalf, C. (2015). Sediment-rich meltwater plumes and ice-proximal fans at the margins of modern and ancient tidewater glaciers: Observations and modelling. Sedimentology, 62(6), 1665-1692. https://doi.org/https://doi.org/10.1111/sed.12198

Drews, R., Pattyn, F., Hewitt, I. J., Ng, F. S. L., Berger, S., Matsuoka, K., Helm, V., Bergeot, N., Favier, L., & Neckel, N. (2017). Actively evolving subglacial conduits and eskers initiate ice shelf channels at an Antarctic grounding line. Nature Communications, 8(1), 15228. https://doi.org/10.1038/ncomms15228

Dupont, T. K., & Alley, R. B. (2005). Assessment of the importance of ice-shelf buttressing to ice-sheet flow. Geophysical Research Letters, 32(4). https://doi.org/https://doi.org/10.1029/2004GL022024

Favier, L., Jourdain, N. C., Jenkins, A., Merino, N., Durand, G., Gagliardini, O., Gillet-Chaulet, F., & Mathiot, P. (2019). Assessment of sub-shelf melting parameterisations using the ocean–ice-sheet coupled model NEMO(v3.6)–Elmer/Ice(v8.3). Geosci. Model Dev., 12(6), 2255-2283. https://doi.org/10.5194/gmd-12-2255-2019

Favier, L., Pattyn, F., Berger, S., & Drews, R. (2016). Dynamic influence of pinning points on marine ice-sheet stability: a numerical study in Dronning Maud Land, East Antarctica. The Cryosphere, 10(6), 2623-2635. https://doi.org/10.5194/tc-10-2623-2016

Freer, B. I. D., Marsh, O. J., Fricker, H. A., Hogg, A. E., Siegfried, M. R., Floricioiu, D., Sauthoff, W., Rigby, R., & Wilson, S. F. (2024). Coincident Lake Drainage and Grounding Line Retreat at Engelhardt Subglacial Lake, West Antarctica. Journal of Geophysical Research: Earth Surface, 129(9), e2024JF007724. https://doi.org/https://doi.org/10.1029/2024JF007724

Fricker, H. A., Galton-Fenzi, B. K., Walker, C. C., Freer, B. I. D., Padman, L., & DeConto, R. (2025). Antarctica in 2025: Drivers of deep uncertainty in projected ice loss. Science, 387(6734), 601-609. https://doi.org/10.1126/science.adt9619

Gadi, R., Rignot, E., & Menemenlis, D. (2023). Modeling Ice Melt Rates From Seawater Intrusions in the Grounding Zone of Petermann Gletscher, Greenland. Geophysical Research Letters, 50(24), e2023GL105869. https://doi.org/https://doi.org/10.1029/2023GL105869

Gandy, N., Gregoire, L. J., Ely, J. C., Cornford, S. L., Clark, C. D., & Hodgson, D. M. (2019). Exploring the ingredients required to successfully model the placement, generation, and evolution of ice streams in the British-Irish Ice Sheet. Quaternary Science Reviews, 223, 105915. https://doi.org/https://doi.org/10.1016/j.quascirev.2019.105915

Gladstone, R. M., Lee, V., Vieli, A., & Payne, A. J. (2010). Grounding line migration in an adaptive mesh ice sheet model. Journal of Geophysical Research: Earth Surface, 115(F4). https://doi.org/https://doi.org/10.1029/2009JF001615

Gladstone, R. M., Warner, R. C., Galton-Fenzi, B. K., Gagliardini, O., Zwinger, T., & Greve, R. (2017). Marine ice sheet model performance depends on basal sliding physics and sub-shelf melting. The Cryosphere, 11(1), 319-329. https://doi.org/10.5194/tc-11-319-2017

Gourmelen, N., Jakob, L., Holland, P. R., Dutrieux, P., Goldberg, D., Bevan, S., Luckman, A., & Malczyk, G. (2025). The influence of subglacial lake discharge on Thwaites Glacier ice-shelf melting and grounding-line retreat. Nature Communications, 16(1), 2272. https://doi.org/10.1038/s41467-025-57417-1

Gudmundsson, G. H. (2003). Transmission of basal variability to a glacier surface. Journal of Geophysical Research: Solid Earth, 108(B5). https://doi.org/https://doi.org/10.1029/2002JB002107

Gudmundsson, G. H. (2007). Tides and the flow of Rutford Ice Stream, West Antarctica. Journal of Geophysical Research: Earth Surface, 112(F4). https://doi.org/https://doi.org/10.1029/2006JF000731

Gudmundsson, G. H. (2013). Ice-shelf buttressing and the stability of marine ice sheets. The Cryosphere, 7(2), 647-655. https://doi.org/10.5194/tc-7-647-2013

Gudmundsson, G. H., Barnes, J. M., Goldberg, D. N., & Morlighem, M. (2023). Limited Impact of Thwaites Ice Shelf on Future Ice Loss From Antarctica. Geophysical Research Letters, 50(11), e2023GL102880. https://doi.org/https://doi.org/10.1029/2023GL102880

Gudmundsson, G. H., Paolo, F. S., Adusumilli, S., & Fricker, H. A. (2019). Instantaneous Antarctic ice sheet mass loss driven by thinning ice shelves. Geophysical Research Letters, 46(23), 13903-13909. https://doi.org/https://doi.org/10.1029/2019GL085027

Gustafson, C. D., Key, K., Siegfried, M. R., Winberry, J. P., Fricker, H. A., Venturelli, R. A., & Michaud, A. B. (2022). A dynamic saline groundwater system mapped beneath an Antarctic ice stream. Science, 376(6593), 640-644. https://doi.org/10.1126/science.abm3301

Gwyther, D. E., Dow, C. F., Jendersie, S., Gourmelen, N., & Galton-Fenzi, B. K. (2023). Subglacial Freshwater Drainage Increases Simulated Basal Melt of the Totten Ice Shelf. Geophysical Research Letters, 50(12), e2023GL103765. https://doi.org/https://doi.org/10.1029/2023GL103765

Hager, A. O., Hoffman, M. J., Price, S. F., & Schroeder, D. M. (2022). Persistent, extensive channelized drainage modeled beneath Thwaites Glacier, West Antarctica. The Cryosphere, 16(9), 3575-3599. https://doi.org/10.5194/tc-16-3575-2022

Hanebuth, T. J. J., Rebesco, M., Urgeles, R., Lucchi, R. G., & Freudenthal, T. (2014). Drilling Glacial Deposits in Offshore Polar Regions. Eos, Transactions American Geophysical Union, 95(31), 277-278. https://doi.org/https://doi.org/10.1002/2014EO310001

Hank, K., Arthern, R. J., Williams, C. R., Brisbourne, A. M., Smith, A. M., Smith, J. A., Wåhlin, A., & Anandakrishnan, S. (2025). The Antarctic Ice Sheet sliding law inferred from seismic observations. EGUsphere, 2025, 1-22. https://doi.org/10.5194/egusphere-2025-764

Hansen, D. D., & Zoet, L. K. (2022). Characterizing Sediment Flux of Deforming Glacier Beds. Journal of Geophysical Research: Earth Surface, 127(4), e2021JF006544. https://doi.org/https://doi.org/10.1029/2021JF006544

Hoffman, A. O., Christianson, K., Holschuh, N., Case, E., Kingslake, J., & Arthern, R. (2022). The Impact of Basal Roughness on Inland Thwaites Glacier Sliding. Geophysical Research Letters, 49(14), e2021GL096564. https://doi.org/https://doi.org/10.1029/2021GL096564

Hofstede, C., Beyer, S., Corr, H., Eisen, O., Hattermann, T., Helm, V., Neckel, N., Smith, E. C., Steinhage, D., Zeising, O., & Humbert, A. (2021). Evidence for a grounding line fan at the onset of a basal channel under the ice shelf of Support Force Glacier, Antarctica, revealed by reflection seismics. The Cryosphere, 15(3), 1517-1535. https://doi.org/10.5194/tc-15-1517-2021

Hogan, K. A., Arnold, N. S., Larter, R. D., Kirkham, J. D., Noormets, R., Ó Cofaigh, C., Golledge, N. R., & Dowdeswell, J. A. (2022). Subglacial Water Flow Over an Antarctic Palaeo-Ice Stream Bed. Journal of Geophysical Research: Earth Surface, 127(2), e2021JF006442. https://doi.org/https://doi.org/10.1029/2021JF006442

Hogan, K. A., Larter, R. D., Graham, A. G. C., Arthern, R., Kirkham, J. D., Totten, R. L., Jordan, T. A., Clark, R., Fitzgerald, V., Wåhlin, A. K., Anderson, J. B., Hillenbrand, C. D., Nitsche, F. O., Simkins, L., Smith, J. A., Gohl, K., Arndt, J. E., Hong, J., & Wellner, J. (2020). Revealing the former bed of Thwaites Glacier using sea-floor bathymetry: implications for warm-water routing and bed controls on ice flow and buttressing. The Cryosphere, 14(9), 2883-2908. https://doi.org/10.5194/tc-14-2883-2020

Holschuh, N., Christianson, K., Paden, J., Alley, R. B., & Anandakrishnan, S. (2020). Linking postglacial landscapes to glacier dynamics using swath radar at Thwaites Glacier, Antarctica. Geology, 48(3), 268-272. https://doi.org/10.1130/G46772.1

Holt, J. W., Blankenship, D. D., Morse, D. L., Young, D. A., Peters, M. E., Kempf, S. D., Richter, T. G., Vaughan, D. G., & Corr, H. F. J. (2006). New boundary conditions for the West Antarctic Ice Sheet: Subglacial topography of the Thwaites and Smith glacier catchments. Geophysical Research Letters, 33(9). https://doi.org/https://doi.org/10.1029/2005GL025561

Horgan, H. J., Alley, R. B., Christianson, K., Jacobel, R. W., Anandakrishnan, S., Muto, A., Beem, L. H., & Siegfried, M. R. (2013). Estuaries beneath ice sheets. Geology, 41(11), 1159-1162. https://doi.org/10.1130/G34654.1

Horgan, H. J., Stewart, C., Stevens, C., Dunbar, G., Balfoort, L., Schmidt, B. E., Washam, P., Werder, M. A., Mandeno, D., Marschalek, J., Hulbe, C., Holschuh, N., Levy, R., Hurwitz, B., Jendersie, S., Johnson, K., Lawrence, J., Morgenstern, R., Mullen, A. D., Quartini, E., Sauthoff, W., Siegfried, M., Still, H., Thorpe-Loersuch, S., van de Fliert, T., Venturelli, R., & Whiteford, A. (2025). A West Antarctic grounding-zone environment shaped by episodic water flow. Nature Geoscience, 18(5), 389-395. https://doi.org/10.1038/s41561-025-01687-3

Horgan, H. J., van Haastrecht, L., Alley, R. B., Anandakrishnan, S., Beem, L. H., Christianson, K., Muto, A., & Siegfried, M. R. (2021). Grounding zone subglacial properties from calibrated active-source seismic methods. The Cryosphere, 15(4), 1863-1880. https://doi.org/10.5194/tc-15-1863-2021

Iverson, N. R., Hooyer, T. S., & Baker, R. W. (1998). Ring-shear studies of till deformation: Coulomb-plastic behavior and distributed strain in glacier beds. Journal of Glaciology, 44(148), 634-642. https://doi.org/10.3189/S0022143000002136

Iverson, N. R., & Iverson, R. M. (2001). Distributed shear of subglacial till due to Coulomb slip. Journal of Glaciology, 47(158), 481-488. https://doi.org/10.3189/172756501781832115

Jordan, T. A., Thompson, S., Kulessa, B., & Ferraccioli, F. Geological sketch map and implications for ice flow of Thwaites Glacier, West Antarctica, from integrated aerogeophysical observations. Science Advances, 9(22), eadf2639. https://doi.org/10.1126/sciadv.adf2639

Joughin, I., Shapero, D., & Dutrieux, P. (2024). Responses of the Pine Island and Thwaites glaciers to melt and sliding parameterizations. The Cryosphere, 18(5), 2583-2601. https://doi.org/10.5194/tc-18-2583-2024

Jourdain, N. C., Asay-Davis, X., Hattermann, T., Straneo, F., Seroussi, H., Little, C. M., & Nowicki, S. (2020). A protocol for calculating basal melt rates in the ISMIP6 Antarctic ice sheet projections. The Cryosphere, 14(9), 3111-3134. https://doi.org/10.5194/tc-14-3111-2020

Kamb, B. (2001). Basal Zone of the West Antarctic Ice Streams and its Role in Lubrication of Their Rapid Motion. In The West Antarctic Ice Sheet: Behavior and Environment (pp. 157-199). https://doi.org/https://doi.org/10.1029/AR077p0157

Kazmierczak, E., Gregov, T., Coulon, V., & Pattyn, F. (2024). A fast and simplified subglacial hydrological model for the Antarctic Ice Sheet and outlet glaciers. The Cryosphere, 18(12), 5887-5911. https://doi.org/10.5194/tc-18-5887-2024

Key, K., & Siegfried, M. R. (2017). The feasibility of imaging subglacial hydrology beneath ice streams with ground-based electromagnetics. Journal of Glaciology, 63(241), 755-771. https://doi.org/10.1017/jog.2017.36

Kirkham, J. D., Hogan, K. A., Larter, R. D., Arnold, N. S., Nitsche, F. O., Golledge, N. R., & Dowdeswell, J. A. (2019). Past water flow beneath Pine Island and Thwaites glaciers, West Antarctica. The Cryosphere, 13(7), 1959-1981. https://doi.org/10.5194/tc-13-1959-2019

Koellner, S., Parizek, B. R., Alley, R. B., Muto, A., & Holschuh, N. (2019). The impact of spatially-variable basal properties on outlet glacier flow. Earth and Planetary Science Letters, 515, 200-208. https://doi.org/https://doi.org/10.1016/j.epsl.2019.03.026

Kubiszewski, I., Adams, V. M., Baird, R., Boothroyd, A., Costanza, R., MacDonald, D. H., Finau, G., Fulton, E. A., King, C. K., King, M. A., Lannuzel, D., Leane, E., Melbourne-Thomas, J., Ooi, C.-S., Raghavan, M., Senigaglia, V., Stoeckl, N., Tian, J., & Yamazaki, S. (2025). Cascading tipping points of Antarctica and the Southern Ocean. Ambio, 54(4), 642-659. https://doi.org/10.1007/s13280-024-02101-9

Larour, E., Seroussi, H., Adhikari, S., Ivins, E., Caron, L., Morlighem, M., & Schlegel, N. (2019). Slowdown in Antarctic mass loss from solid Earth and sea-level feedbacks. Science, 364(6444), eaav7908. https://doi.org/10.1126/science.aav7908

Larour, E., Seroussi, H., Adhikari, S., Ivins, E., Caron, L., Morlighem, M., & Schlegel, N. (2019). Slowdown in Antarctic mass loss from solid Earth and sea-level feedbacks. Science, 364(6444), eaav7908. https://doi.org/10.1126/science.aav7908

Larter, R. D., & Vanneste, L. E. (1995). Relict subglacial deltas on the Antarctic Peninsula outer shelf. *Geology*, *23*(1), 33-36. https://doi.org/10.1130/0091-7613(1995)023<0033:RSDOTA>2.3.CO;2

Laskar, J., Robutel, P., Joutel, F., Gastineau, M., Correia, A. C. M., & Levrard, B. (2004). A long-term numerical solution for the insolation quantities of the Earth [10.1051/0004-6361:20041335]. A&A, 428(1), 261-285. https://doi.org/10.1051/0004-6361:20041335

Le Brocq, A. M., Ross, N., Griggs, J. A., Bingham, R. G., Corr, H. F. J., Ferraccioli, F., Jenkins, A., Jordan, T. A., Payne, A. J., Rippin, D. M., & Siegert, M. J. (2013). Evidence from ice shelves for channelized meltwater flow beneath the Antarctic Ice Sheet. Nature Geoscience, 6(11), 945-948. https://doi.org/10.1038/ngeo1977

Leguy, G. R., Asay-Davis, X. S., & Lipscomb, W. H. (2014). Parameterization of basal friction near grounding lines in a one-dimensional ice sheet model. The Cryosphere, 8(4), 1239-1259. https://doi.org/10.5194/tc-8-1239-2014

Leguy, G. R., Lipscomb, W. H., & Asay-Davis, X. S. (2021). Marine ice sheet experiments with the Community Ice Sheet Model. The Cryosphere, 15(7), 3229-3253. https://doi.org/10.5194/tc-15-3229-2021

Li, X., Rignot, E., Morlighem, M., Mouginot, J., & Scheuchl, B. (2015). Grounding line retreat of Totten Glacier, East Antarctica, 1996 to 2013. Geophysical Research Letters, 42(19), 8049-8056. https://doi.org/https://doi.org/10.1002/2015GL065701

Malczyk, G., Gourmelen, N., Goldberg, D., Wuite, J., & Nagler, T. (2020). Repeat Subglacial Lake Drainage and Filling Beneath Thwaites Glacier. Geophysical Research Letters, 47(23), e2020GL089658. https://doi.org/https://doi.org/10.1029/2020GL089658

Mamer, M. S., Robel, A. A., Lai, C. C. K., Wilson, E., & Washam, P. (2025). Modeling mixing and melting in laminar seawater intrusions under grounded ice. The Cryosphere, 19(8), 3227-3251. https://doi.org/10.5194/tc-19-3227-2025

Martin, M. A., Winkelmann, R., Haseloff, M., Albrecht, T., Bueler, E., Khroulev, C., & Levermann, A. (2011). The Potsdam Parallel Ice Sheet Model (PISM-PIK) – Part 2: Dynamic equilibrium simulation of the Antarctic ice sheet. The Cryosphere, 5(3), 727-740. https://doi.org/10.5194/tc-5-727-2011

McMullen, K., Domack, E., Leventer, A., Olson, C., Dunbar, R., & Brachfeld, S. (2006). Glacial morphology and sediment formation in the Mertz Trough, East Antarctica. Palaeogeography, Palaeoclimatology, Palaeoecology, 231(1), 169-180. https://doi.org/https://doi.org/10.1016/j.palaeo.2005.08.004

Meyer, C. R., Warburton, K. L. P., Sommers, A. N., & Minchew, B. M. (2025). Influence of water extraction on subglacial hydrology and glacier velocity. EGUsphere, 2025, 1-29. https://doi.org/10.5194/egusphere-2025-4867

Milillo, P., Rignot, E., Rizzoli, P., Scheuchl, B., Mouginot, J., Bueso-Bello, J., & Prats-Iraola, P. (2019). Heterogeneous retreat and ice melt of Thwaites Glacier, West Antarctica. Science Advances, 5(1), eaau3433. https://doi.org/10.1126/sciadv.aau3433

Milillo, P., Rignot, E., Rizzoli, P., Scheuchl, B., Mouginot, J., Bueso-Bello, J. L., Prats-Iraola, P., & Dini, L. (2022). Rapid glacier retreat rates observed in West Antarctica. Nature Geoscience, 15(1), 48-53. https://doi.org/10.1038/s41561-021-00877-z

Minchew, B. M., Simons, M., Riel, B., & Milillo, P. (2017). Tidally induced variations in vertical and horizontal motion on Rutford Ice Stream, West Antarctica, inferred from remotely sensed observations. Journal of Geophysical Research: Earth Surface, 122(1), 167-190. https://doi.org/https://doi.org/10.1002/2016JF003971

Mohajerani, Y., Jeong, S., Scheuchl, B., Velicogna, I., Rignot, E., & Milillo, P. (2021). Automatic delineation of glacier grounding lines in differential interferometric synthetic-aperture radar data using deep learning. Scientific Reports, 11(1), 4992. https://doi.org/10.1038/s41598-021-84309-3

Nakayama, Y., Cai, C., & Seroussi, H. (2021). Impact of Subglacial Freshwater Discharge on Pine Island Ice Shelf. Geophysical Research Letters, 48(18), e2021GL093923. https://doi.org/https://doi.org/10.1029/2021GL093923

Ó Cofaigh, C., Dowdeswell, J. A., Allen, C. S., Hiemstra, J. F., Pudsey, C. J., Evans, J., & J.A. Evans, D. (2005). Flow dynamics and till genesis associated with a marine-based Antarctic palaeo-ice stream. Quaternary Science Reviews, 24(5), 709-740. https://doi.org/https://doi.org/10.1016/j.quascirev.2004.10.006

O'Brien, P. E., Santis, L. D., Harris, P. T., Domack, E., & Quilty, P. G. (1999). Ice shelf grounding zone features of western Prydz Bay, Antarctica: sedimentary processes from seismic and sidescan images. Antarctic Science, 11(1), 78-91. https://doi.org/10.1017/S0954102099000115

Parizek, B. R. (2024). Grounding Zones: The “Inland” Dynamic Interface Between Seawater, Outlet Glaciers, Subglacial Meltwater Routing, and Ice-Shelf Processes. Geophysical Research Letters, 51(15), e2024GL110427. https://doi.org/https://doi.org/10.1029/2024GL110427

Parizek, B. R., Christianson, K., Anandakrishnan, S., Alley, R. B., Walker, R. T., Edwards, R. A., Wolfe, D. S., Bertini, G. T., Rinehart, S. K., Bindschadler, R. A., & Nowicki, S. M. J. (2013). Dynamic (in)stability of Thwaites Glacier, West Antarctica. Journal of Geophysical Research: Earth Surface, 118(2), 638-655. https://doi.org/https://doi.org/10.1002/jgrf.20044

Pattyn, F., & Morlighem, M. (2020). The uncertain future of the Antarctic Ice Sheet. Science, 367(6484), 1331-1335. https://doi.org/10.1126/science.aaz5487

Pattyn, F., Schoof, C., Perichon, L., Hindmarsh, R. C. A., Bueler, E., de Fleurian, B., Durand, G., Gagliardini, O., Gladstone, R., Goldberg, D., Gudmundsson, G. H., Huybrechts, P., Lee, V., Nick, F. M., Payne, A. J., Pollard, D., Rybak, O., Saito, F., & Vieli, A. (2012). Results of the Marine Ice Sheet Model Intercomparison Project, MISMIP. The Cryosphere, 6(3), 573-588. https://doi.org/10.5194/tc-6-573-2012

Pelle, T., Greenbaum, J. S., Ehrenfeucht, S., Dow, C. F., & McCormack, F. S. (2024). Subglacial Discharge Accelerates Dynamic Retreat of Aurora Subglacial Basin Outlet Glaciers, East Antarctica, Over the 21st Century. Journal of Geophysical Research: Earth Surface, 129(7), e2023JF007513. https://doi.org/https://doi.org/10.1029/2023JF007513

Pollard, D., & DeConto, R. M. (2012). A simple inverse method for the distribution of basal sliding coefficients under ice sheets, applied to Antarctica. The Cryosphere, 6(5), 953-971. https://doi.org/10.5194/tc-6-953-2012

Pollard, D., & DeConto, R. M. (2020). Continuous simulations over the last 40 million years with a coupled Antarctic ice sheet-sediment model. Palaeogeography, Palaeoclimatology, Palaeoecology, 537, 109374. https://doi.org/https://doi.org/10.1016/j.palaeo.2019.109374

Powell, R. D., Dawber, M., McInnes, J. N., & Pyne, A. R. (1996). Observations of the grounding-line area at a floating glacier terminus. Annals of Glaciology, 22, 217-223. https://doi.org/10.3189/1996AoG22-1-217-223

Powell, R. D., Dawber, M., McInnes, J. N., & Pyne, A. R. (1996). Observations of the grounding-line area at a floating glacier terminus. Annals of Glaciology, 22, 217-223. https://doi.org/10.3189/1996AoG22-1-217-223

Powell Ross, D. (1990). Glacimarine processes at grounding-line fans and their growth to ice-contact deltas. Geological Society, London, Special Publications, 53(1), 53-73. https://doi.org/10.1144/GSL.SP.1990.053.01.03

Prior-Jones, M., Jonathan, H., Craw, L., Bagshaw, E. A., Dow, C. F., Mason-Jones, A., Alnader, H., von Benzon, E., Copland, L., Dahl-Jensen, D., Main, B., James, J., Livingstone, S., Mann, S., Peacey, M., Perkins, R., & Rahn, S. M. (2025/04/1). Cryoegg, Cryowurst and Hydrobean: wireless instruments for glaciology and hydrology.

Pritchard, H. D., Fretwell, P. T., Fremand, A. C., Bodart, J. A., Kirkham, J. D., Aitken, A., Bamber, J., Bell, R., Bianchi, C., Bingham, R. G., Blankenship, D. D., Casassa, G., Christianson, K., Conway, H., Corr, H. F. J., Cui, X., Damaske, D., Damm, V., Dorschel, B., . . . Zirizzotti, A. (2025). Bedmap3 updated ice bed, surface and thickness gridded datasets for Antarctica. Scientific Data, 12(1), 414. https://doi.org/10.1038/s41597-025-04672-y

Pritchard, H. D., Fretwell, P. T., Fremand, A. C., Bodart, J. A., Kirkham, J. D., Aitken, A., Bamber, J., Bell, R., Bianchi, C., Bingham, R. G., Blankenship, D. D., Casassa, G., Christianson, K., Conway, H., Corr, H. F. J., Cui, X., Damaske, D., Damm, V., Dorschel, B., . . . Zirizzotti, A. (2025). Bedmap3 updated ice bed, surface and thickness gridded datasets for Antarctica. Scientific Data, 12(1), 414. https://doi.org/10.1038/s41597-025-04672-y

Pritchard, H. D., Ligtenberg, S. R. M., Fricker, H. A., Vaughan, D. G., van den Broeke, M. R., & Padman, L. (2012). Antarctic ice-sheet loss driven by basal melting of ice shelves. Nature, 484(7395), 502-505. https://doi.org/10.1038/nature10968

Reese, R., Winkelmann, R., & Gudmundsson, G. H. (2018). Grounding-line flux formula applied as a flux condition in numerical simulations fails for buttressed Antarctic ice streams. The Cryosphere, 12(10), 3229-3242. https://doi.org/10.5194/tc-12-3229-2018

Rignot, E. (2023). Observations of grounding zones are the missing key to understand ice melt in Antarctica. Nature Climate Change, 13(10), 1010-1013. https://doi.org/10.1038/s41558-023-01819-w

Rignot, E., Ciracì, E., Scheuchl, B., Tolpekin, V., Wollersheim, M., & Dow, C. (2024). Widespread seawater intrusions beneath the grounded ice of Thwaites Glacier, West Antarctica. Proceedings of the National Academy of Sciences, 121(22), e2404766121. https://doi.org/10.1073/pnas.2404766121

Rignot, E., Mouginot, J., Morlighem, M., Seroussi, H., & Scheuchl, B. (2014). Widespread, rapid grounding line retreat of Pine Island, Thwaites, Smith, and Kohler glaciers, West Antarctica, from 1992 to 2011. Geophysical Research Letters, 41(10), 3502-3509. https://doi.org/https://doi.org/10.1002/2014GL060140

Rignot, E., Mouginot, J., & Scheuchl, B. (2011). Antarctic grounding line mapping from differential satellite radar interferometry. Geophysical Research Letters, 38(10). https://doi.org/https://doi.org/10.1029/2011GL047109

Rignot, E., Mouginot, J., & Scheuchl, B. (2017). MEaSUREs InSAR-Based Antarctica Ice Velocity Map, Version 2 NASA National Snow and Ice Data Center Distributed Active Archive Center. https://doi.org/10.5067/D7GK8F5J8M8R

Robel, A. A., Wilson, E., & Seroussi, H. (2022). Layered seawater intrusion and melt under grounded ice. The Cryosphere, 16(2), 451-469. https://doi.org/10.5194/tc-16-451-2022

Robel, A. A., Wilson, E., & Seroussi, H. (2022). Layered seawater intrusion and melt under grounded ice. The Cryosphere, 16(2), 451-469. https://doi.org/10.5194/tc-16-451-2022

Roseby, Z. A., Smith, J. A., Hillenbrand, C.-D., Cartigny, M. J. B., Rosenheim, B. E., Hogan, K. A., Allen, C. S., Leventer, A., Kuhn, G., Ehrmann, W., & Larter, R. D. (2022). History of Anvers-Hugo Trough, western Antarctic Peninsula shelf, since the Last Glacial Maximum. Part I: Deglacial history based on new sedimentological and chronological data. Quaternary Science Reviews, 291, 107590. https://doi.org/https://doi.org/10.1016/j.quascirev.2022.107590

Rosier, S. H. R., Gudmundsson, G. H., King, M. A., Nicholls, K. W., Makinson, K., & Corr, H. F. J. (2017). Strong tidal variations in ice flow observed across the entire Ronne Ice Shelf and adjoining ice streams. Earth Syst. Sci. Data, 9(2), 849-860. https://doi.org/10.5194/essd-9-849-2017

Schmidt, B. E., Washam, P., Davis, P. E. D., Nicholls, K. W., Holland, D. M., Lawrence, J. D., Riverman, K. L., Smith, J. A., Spears, A., Dichek, D. J. G., Mullen, A. D., Clyne, E., Yeager, B., Anker, P., Meister, M. R., Hurwitz, B. C., Quartini, E. S., Bryson, F. E., Basinski-Ferris, A., . . . Makinson, K. (2023). Heterogeneous melting near the Thwaites Glacier grounding line. Nature, 614(7948), 471-478. https://doi.org/10.1038/s41586-022-05691-0

Schoof, C. (2002). Basal perturbations under ice streams: form drag and surface expression. Journal of Glaciology, 48(162), 407-416. https://doi.org/10.3189/172756502781831269

Schoof, C. (2005). The effect of cavitation on glacier sliding. Proceedings of the Royal Society A: Mathematical, Physical and Engineering Sciences, 461(2055), 609-627. https://doi.org/10.1098/rspa.2004.1350

Schoof, C. (2007). Ice sheet grounding line dynamics: Steady states, stability, and hysteresis. Journal of Geophysical Research: Earth Surface, 112(F3). https://doi.org/https://doi.org/10.1029/2006JF000664

Schroeder, D. M., Grima, C., & Blankenship, D. D. (2015). Evidence for variable grounding-zone and shear-margin basal conditions across Thwaites Glacier, West Antarctica. Geophysics, 81(1), WA35-WA43. https://doi.org/10.1190/geo2015-0122.1

Schwans, E., Parizek, B. R., Alley, R. B., Anandakrishnan, S., & Morlighem, M. M. (2023). Model insights into bed control on retreat of Thwaites Glacier, West Antarctica. Journal of Glaciology, 69(277), 1241-1259. https://doi.org/10.1017/jog.2023.13

Seroussi, H., & Morlighem, M. (2018). Representation of basal melting at the grounding line in ice flow models. The Cryosphere, 12(10), 3085-3096. https://doi.org/10.5194/tc-12-3085-2018

Seroussi, H., Nakayama, Y., Larour, E., Menemenlis, D., Morlighem, M., Rignot, E., & Khazendar, A. (2017). Continued retreat of Thwaites Glacier, West Antarctica, controlled by bed topography and ocean circulation. Geophysical Research Letters, 44(12), 6191-6199. https://doi.org/https://doi.org/10.1002/2017GL072910

Siegert, M. J., Kulessa, B., Bougamont, M., Christoffersen, P., Key, K., Andersen, K. R., Booth, A. D., & Smith, A. M. (2018). Antarctic subglacial groundwater: a concept paper on its measurement and potential influence on ice flow. In M. J. Siegert, S. S. R. Jamieson, & D. A. White (Eds.), Exploration of Subsurface Antarctica: Uncovering Past Changes and Modern Processes (Vol. 461, pp. 0). Geological Society of London. https://doi.org/10.1144/SP461.8

Siegert, M. J., Ross, N., Li, J., Schroeder, D. M., Rippin, D., Ashmore, D., Bingham, R., & Gogineni, P. (2016). Subglacial controls on the flow of Institute Ice Stream, West Antarctica. Annals of Glaciology, 57(73), 19-24. https://doi.org/10.1017/aog.2016.17

Sommers, A., Rajaram, H., & Morlighem, M. (2018). SHAKTI: Subglacial Hydrology and Kinetic, Transient Interactions v1.0. Geosci. Model Dev., 11(7), 2955-2974. https://doi.org/10.5194/gmd-11-2955-2018

Sun, S., Pattyn, F., Simon, E. G., Albrecht, T., Cornford, S., Calov, R., Dumas, C., Gillet-Chaulet, F., Goelzer, H., Golledge, N. R., Greve, R., Hoffman, M. J., Humbert, A., Kazmierczak, E., Kleiner, T., Leguy, G. R., Lipscomb, W. H., Martin, D., Morlighem, M., . . . Zhang, T. (2020). Antarctic ice sheet response to sudden and sustained ice-shelf collapse (ABUMIP). Journal of Glaciology, 66(260), 891-904. https://doi.org/10.1017/jog.2020.67

Thomas, R. H. (1979). The Dynamics of Marine Ice Sheets. Journal of Glaciology, 24(90), 167-177. https://doi.org/10.3189/S0022143000014726

Tsai, V. C., Stewart, A. L., & Thompson, A. F. (2015). Marine ice-sheet profiles and stability under Coulomb basal conditions. Journal of Glaciology, 61(226), 205-215. https://doi.org/10.3189/2015JoG14J221

Urlaub, M., Talling, P. J., Zervos, A., & Masson, D. (2015). What causes large submarine landslides on low gradient (<2°) continental slopes with slow (~0.15 m/kyr) sediment accumulation? Journal of Geophysical Research: Solid Earth, 120(10), 6722-6739. https://doi.org/https://doi.org/10.1002/2015JB012347

van den Akker, T., Lipscomb, W. H., Leguy, G. R., van de Berg, W. J., & van de Wal, R. S. W. (2026). Competing processes determine the long-term impact of basal friction parameterizations for Antarctic mass loss. The Cryosphere, 20(2), 1217-1235. https://doi.org/10.5194/tc-20-1217-2026

van Wessem, J. M., van de Berg, W. J., & van den Broeke, M. R. (2023). Data set: Monthly averaged RACMO2.3p2 variables (1979-2022); Antarctica [Data set]. https://doi.org/10.5281/zenodo.7845736

Vaughan, D. G. (1995). Tidal flexure at ice shelf margins. Journal of Geophysical Research: Solid Earth, 100(B4), 6213-6224. https://doi.org/https://doi.org/10.1029/94JB02467

Vaughan, D. G., & Arthern, R. (2007). Why Is It Hard to Predict the Future of Ice Sheets? Science, 315(5818), 1503-1504. https://doi.org/10.1126/science.1141111

Vieli, A., & Payne, A. J. (2005). Assessing the ability of numerical ice sheet models to simulate grounding line migration. Journal of Geophysical Research: Earth Surface, 110(F1). https://doi.org/https://doi.org/10.1029/2004JF000202

Walker, R. T., Parizek, B. R., Alley, R. B., Anandakrishnan, S., Riverman, K. L., & Christianson, K. (2013). Ice-shelf tidal flexure and subglacial pressure variations. Earth and Planetary Science Letters, 361, 422-428. https://doi.org/https://doi.org/10.1016/j.epsl.2012.11.008

Warburton, K. L. P., Hewitt, D. R., & Neufeld, J. A. (2020). Tidal Grounding-Line Migration Modulated by Subglacial Hydrology. Geophysical Research Letters, 47(17), e2020GL089088. https://doi.org/https://doi.org/10.1029/2020GL089088

Warburton, K. L. P., Hewitt, D. R., & Neufeld, J. A. (2023). Shear dilation of subglacial till results in time-dependent sliding laws. Proceedings of the Royal Society A: Mathematical, Physical and Engineering Sciences, 479(2269), 20220536. https://doi.org/10.1098/rspa.2022.0536

Weertman, J. (1957). On the Sliding of Glaciers. Journal of Glaciology, 3(21), 33-38. https://doi.org/10.3189/S0022143000024709

Weertman, J. (1974). Stability of the Junction of an Ice Sheet and an Ice Shelf. Journal of Glaciology, 13(67), 3-11. https://doi.org/10.3189/S0022143000023327

Werder, M. A., Hewitt, I. J., Schoof, C. G., & Flowers, G. E. (2013). Modeling channelized and distributed subglacial drainage in two dimensions. Journal of Geophysical Research: Earth Surface, 118(4), 2140-2158. https://doi.org/https://doi.org/10.1002/jgrf.20146

Wernecke, A., Edwards, T. L., Holden, P. B., Edwards, N. R., & Cornford, S. L. (2022). Quantifying the Impact of Bedrock Topography Uncertainty in Pine Island Glacier Projections for This Century. Geophysical Research Letters, 49(6), e2021GL096589. https://doi.org/https://doi.org/10.1029/2021GL096589

Whillans, I. M., & van der Veen, C. J. (1997). The role of lateral drag in the dynamics of Ice Stream B, Antarctica. Journal of Glaciology, 43(144), 231-237. https://doi.org/10.3189/S0022143000003178

Whiteford, A., Horgan, H. J., Leong, W. J., & Forbes, M. (2022). Melting and Refreezing in an Ice Shelf Basal Channel at the Grounding Line of the Kamb Ice Stream, West Antarctica. Journal of Geophysical Research: Earth Surface, 127(11), e2021JF006532. https://doi.org/https://doi.org/10.1029/2021JF006532

Wilson, E. A., Wells, A. J., Hewitt, I. J., & Cenedese, C. (2020). The dynamics of a subglacial salt wedge. Journal of Fluid Mechanics, 895, A20, Article A20. https://doi.org/10.1017/jfm.2020.308

Wilson, S. F., Hogg, A. E., Rigby, R., Gourmelen, N., Nias, I., & Slater, T. (2025). Detection of 85 new active subglacial lakes in Antarctica from a decade of CryoSat-2 data. Nature Communications, 16(1), 8311. https://doi.org/10.1038/s41467-025-63773-9

Wingham, D. J., Siegert, M. J., Shepherd, A., & Muir, A. S. (2006). Rapid discharge connects Antarctic subglacial lakes. Nature, 440(7087), 1033-1036. https://doi.org/10.1038/nature04660

Zoet, L. K., & Iverson, N. R. (2020). A slip law for glaciers on deformable beds. Science, 368(6486), 76-78. https://doi.org/10.1126/science.aaz1183

Zoet, L. K., Iverson, N. R., Andrews, L., & Helanow, C. (2022). Transient evolution of basal drag during glacier slip. Journal of Glaciology, 68(270), 741-750. https://doi.org/10.1017/jog.2021.131

Supplementary Information for: "Rethinking grounding-zone basal drag for improved projections of Antarctic ice loss"

K. A. Hogan[1], J. A. Neufeld[2], C. Martín[1], M. Mas e Braga[1], A. M. Brisbourne[1], B. Kulessa[3], K. L. P. Warburton[2], J. D. Kirkham[1], O. J. Marsh[1], N. Holschuh[4], K. Christianson[5], J. Paden[6], C. Berndt[7], and R. D. Larter[1]

[1] British Antarctic Survey, High Cross, Madingley Road, Cambridge, CB3 0ET, UK
[2] Department of Applied Mathematics and Theoretical Physics, University of Cambridge, Wilberforce Road, Cambridge CB3 0WA, UK
[3] Glaciology Group, College of Science, Swansea University, Singleton Park, Swansea SA2 8PP, UK
[4] Department of Geology, Amherst College, Amherst, Massachusetts 01002-5000, USA
[5] Department of Earth and Space Sciences, University of Washington, Seattle, Washington 98195-1310, USA
[6] Center for Remote Sensing of Ice Sheets, University of Kansas, Lawrence, Kansas 66045, USA
[7] GEOMAR Helmholtz Centre for Ocean Research, Wischhofstrasse 1-3, D-24148 Kiel, Germany

Correspondence to: Kelly A. Hogan (kelgan@bas.ac.uk)

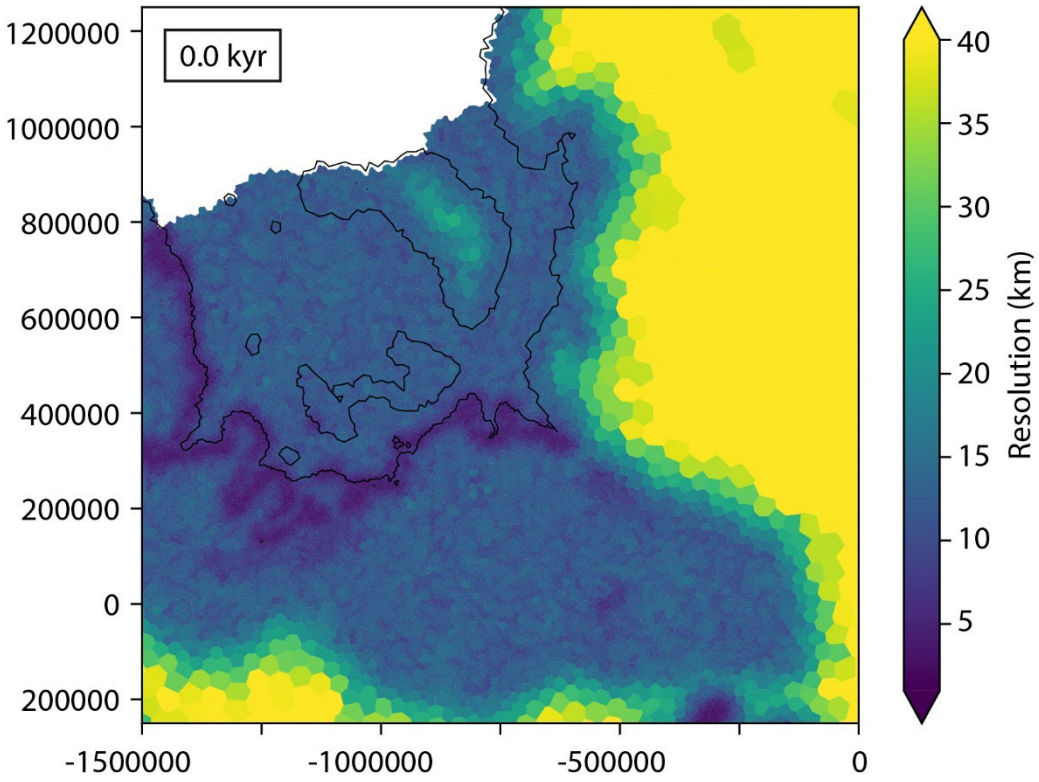

Supplementary Figure S1: UFEMISM mesh resolution for the Weddell Sea ice ice streams at time-step 0 years (present-day). Black is the modelled position of the present-day grounding line.

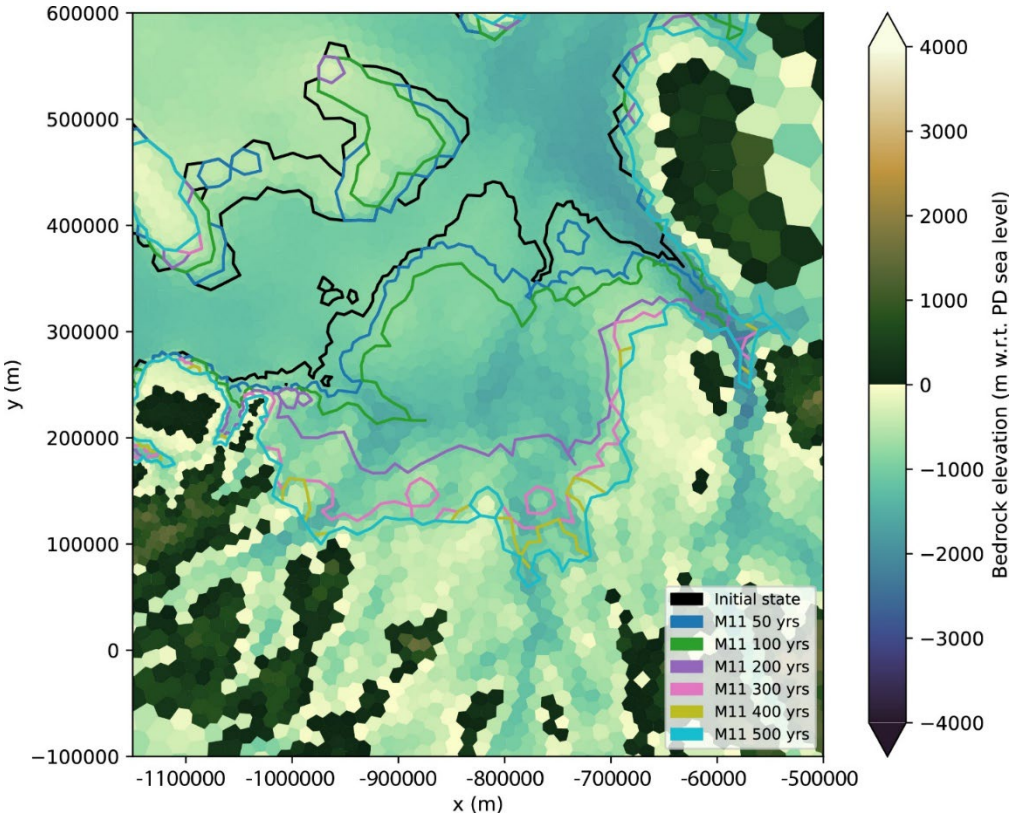

1620

Supplementary Figure S2: Retreated grounding-line positions for the Weddell Sea ice streams overlain on the bed topography for the M11 UFEMISM model run in Section 6.

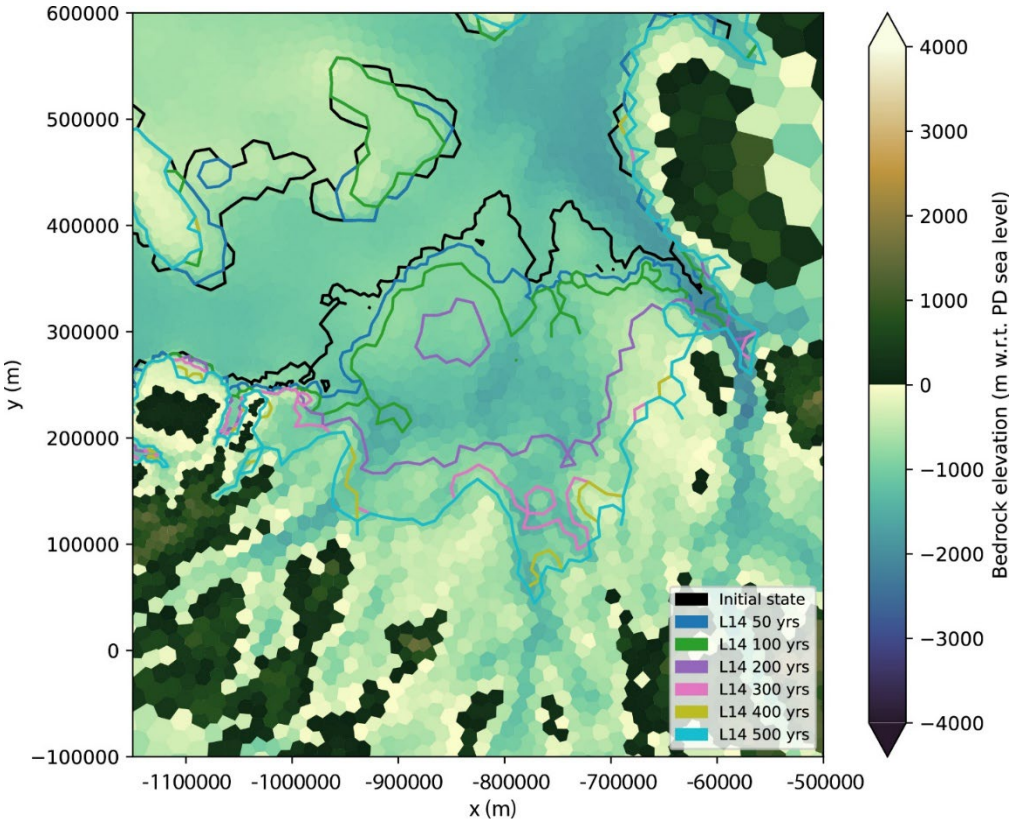

Supplementary Figure S3: Retreated grounding-line (GL) positions for the Weddell Sea ice streams overlain on the bed topography for the L14 UFEMISM model run in Section 6. Compare, for example, the positions of the GL at 300 years (pink line) in this experiment, with the M11 experiment in Figure S2. The L14 GL retreats farther than the M11 GL at this time-step.

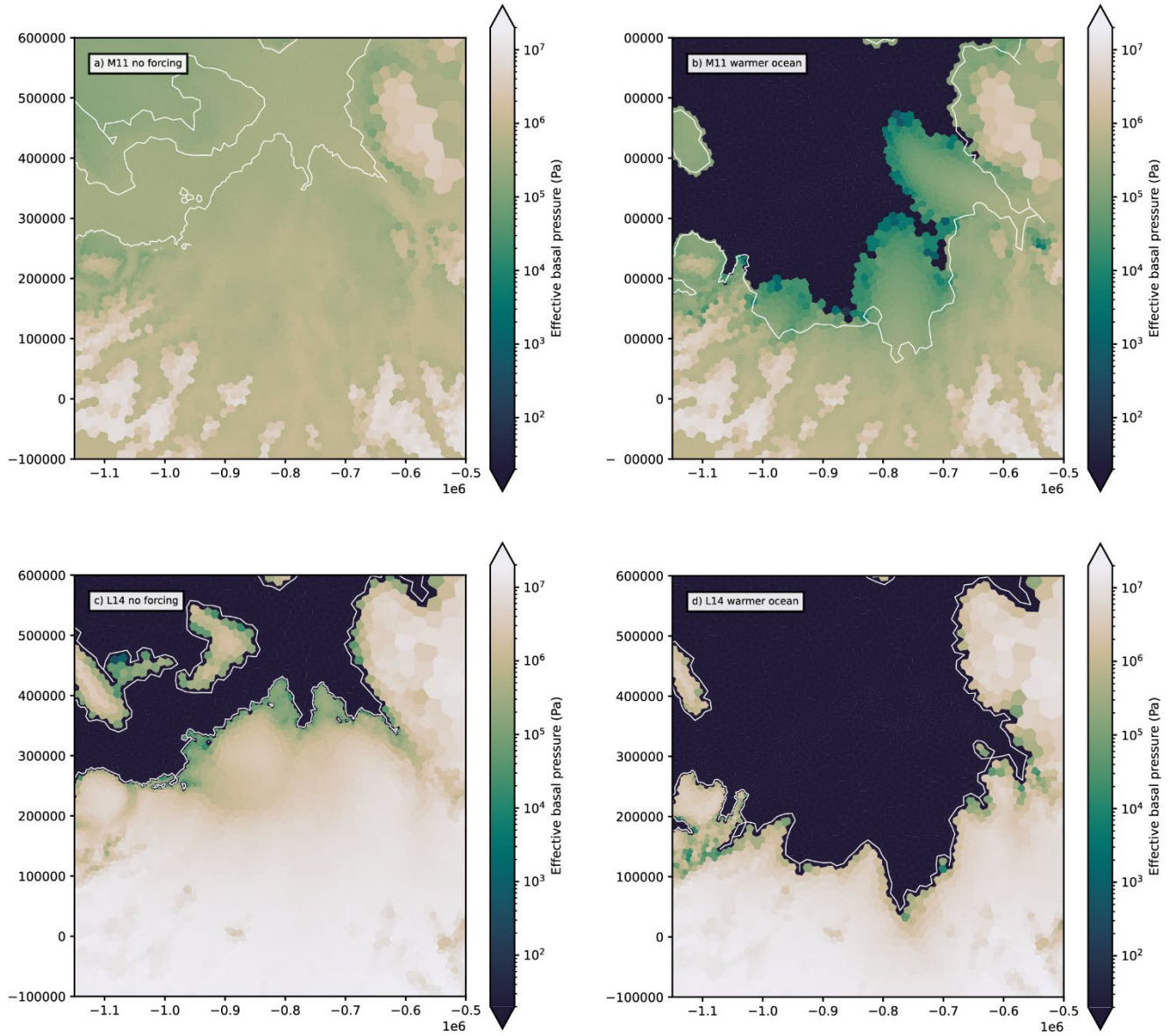

Supplementary Figure S4: Effective pressure, *N*, as modelled in the UFEMISM model for (a) M11 treatment of *N* with no forcing; (b) and with the warmer-ocean forcing; (c) L14 treatment of *N* with no forcing; (d) and with the warmer-ocean forcing.

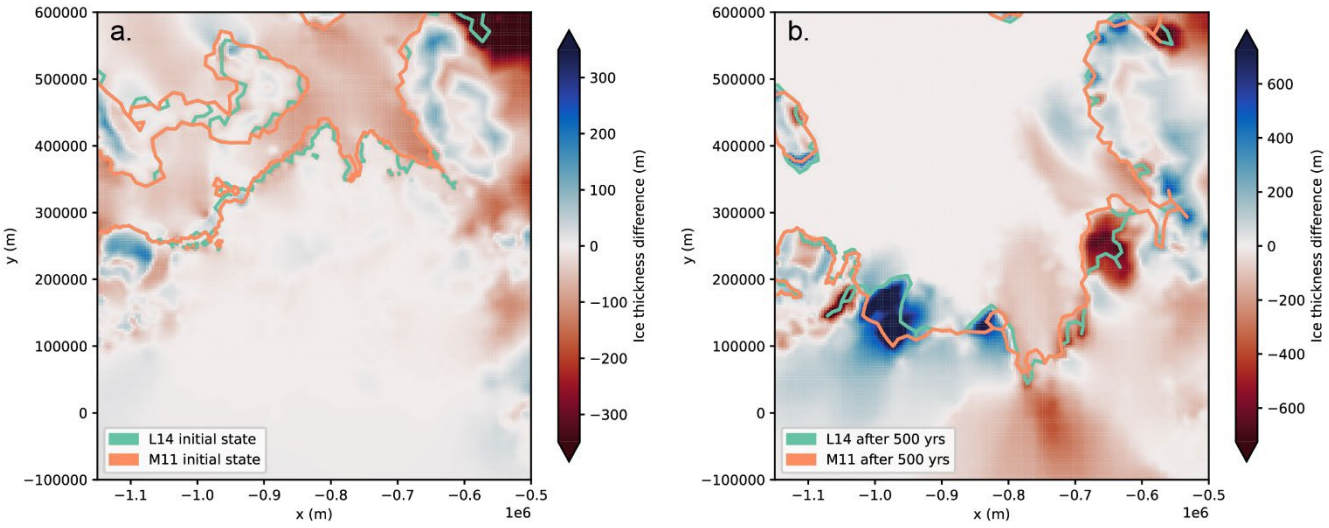

Supplementary Figure S5: Ice thickness differences between the M11 and L14 model runs for (a) the initial state at 0 years; (b) after 500 years. Note the large differences in ice thickness for each treatment of *N* ranging from ~600 m increase in thickness in the Institute catchment, to a 500-600 m difference in the east of the area; note also that the ice thickness differences extend far inland of the modelled grounding lines.

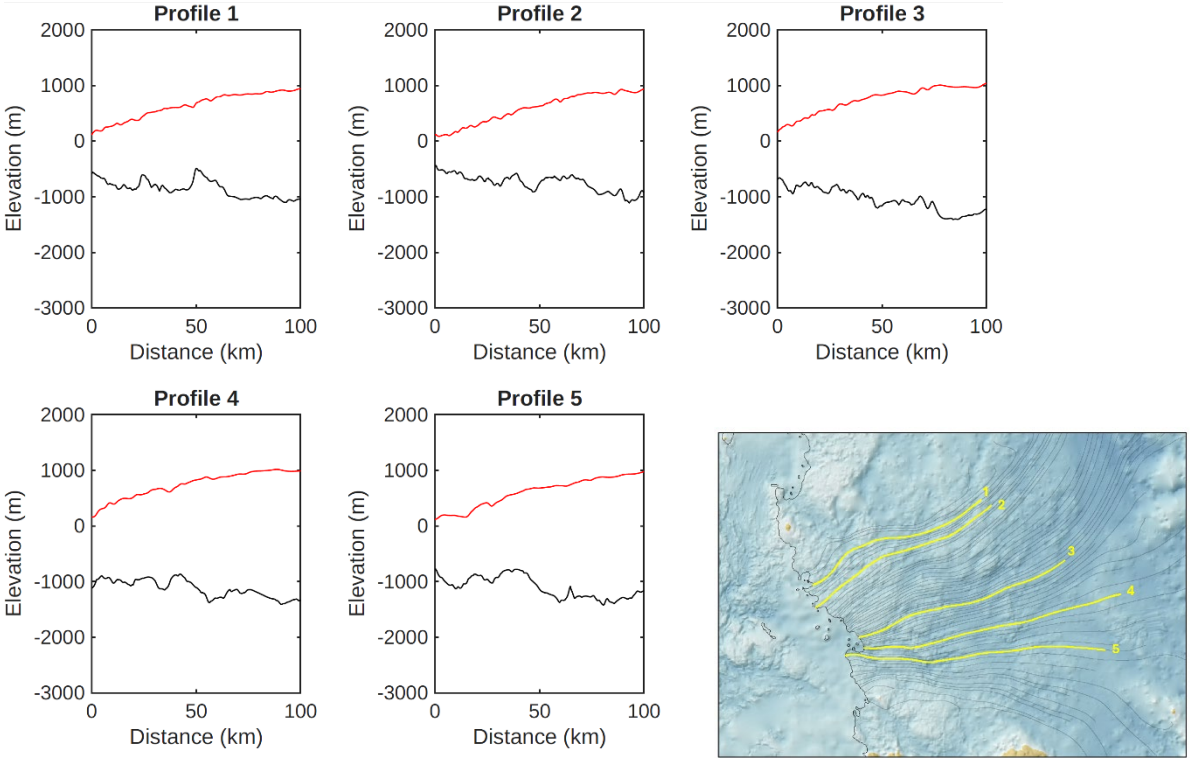

Supplementary Figure S6: Five bed and surface profiles for Thwaites Glacier, Amundsen Sea, extending 100 km up-glacier from the grounding line, along flowlines (for locations see map in bottom right corner). The profile data and flowlines are from the Bedmap3 datasets (Pritchard et al., 2025).

1660

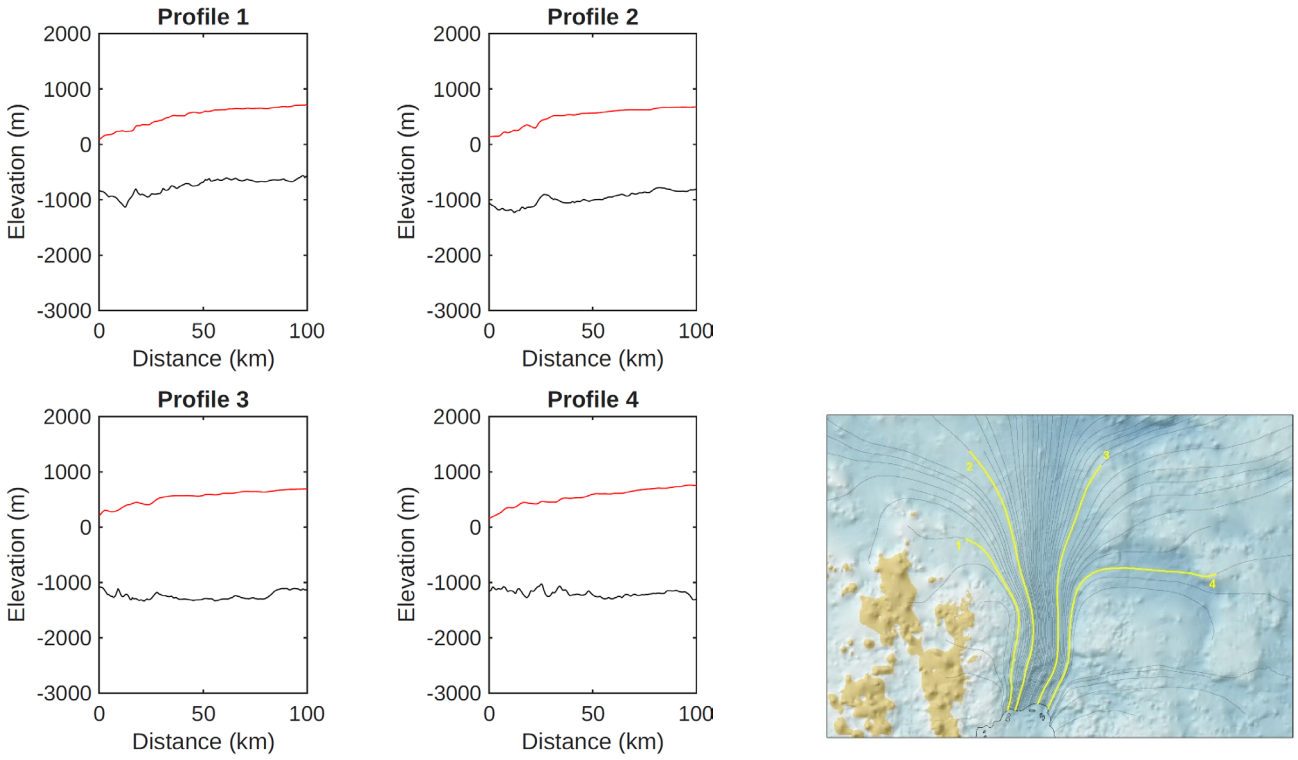

Supplementary Figure S7: Four bed and surface profiles for Pine Island Glacier, Amundsen Sea, extending 100 km up-glacier from the grounding line, along flowlines (for locations see map in bottom right corner). The profile data and flowlines are from the Bedmap3 datasets (Pritchard et al., 2025).

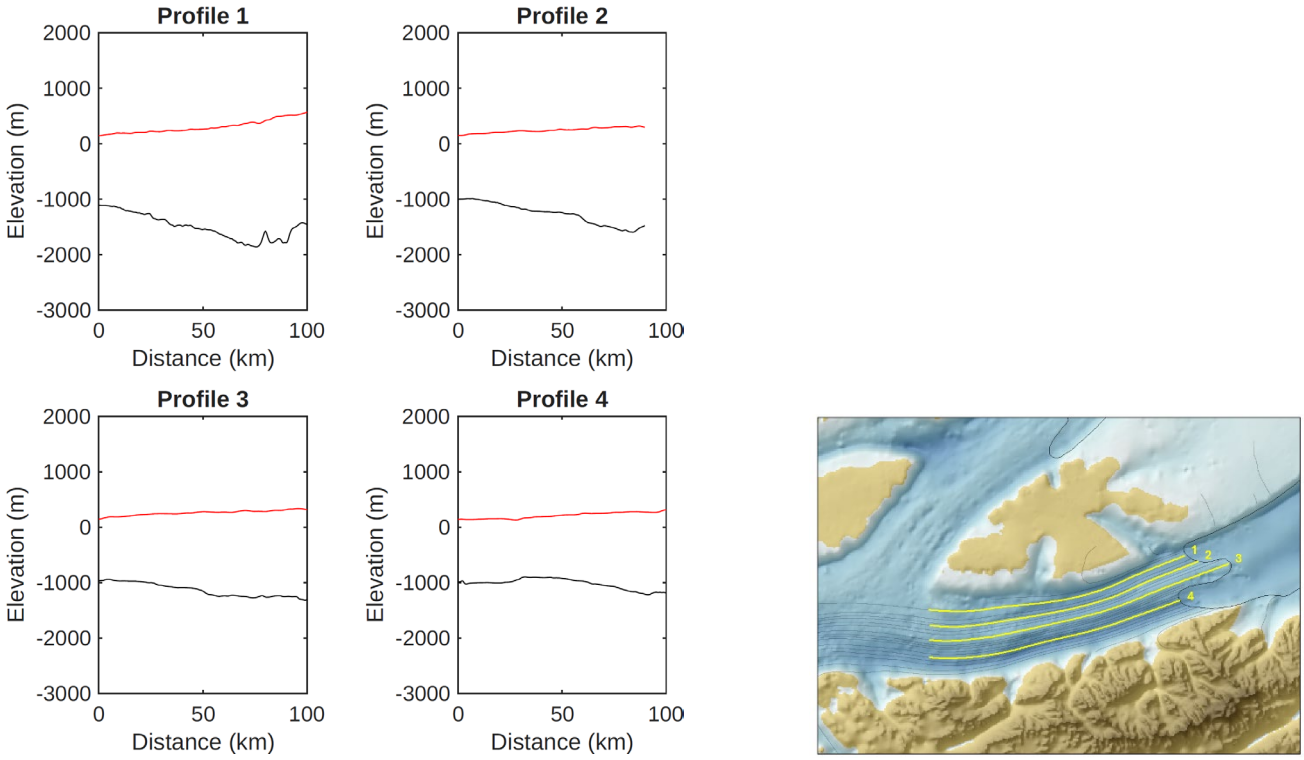

Supplementary Figure S8: Four bed and surface profiles for Rutford Ice Stream, Weddell Sea, extending 100 km up-glacier from the grounding line, along flowlines (for locations see map in bottom right corner). The profile data and flowlines are from the Bedmap3 datasets (Pritchard et al., 2025).

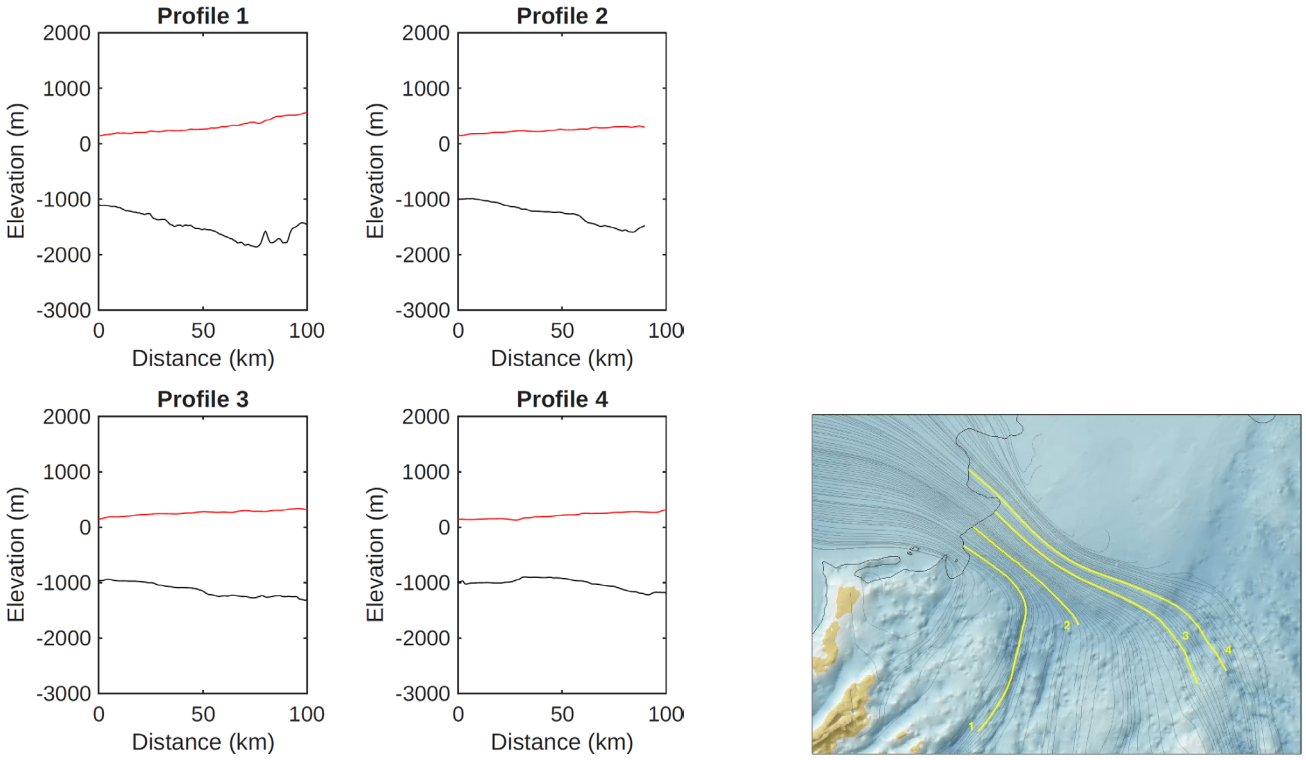

Supplementary Figure S9: Four bed and surface profiles for Institute Ice Stream, Weddell Sea, extending 100 km up-glacier from the grounding line, along flowlines (for locations see map in bottom right corner). The profile data and flowlines are from the Bedmap3 datasets (Pritchard et al., 2025). Note the possible grounding-zone wedge deposit at ~30 km on the bed profile for Profile 4.

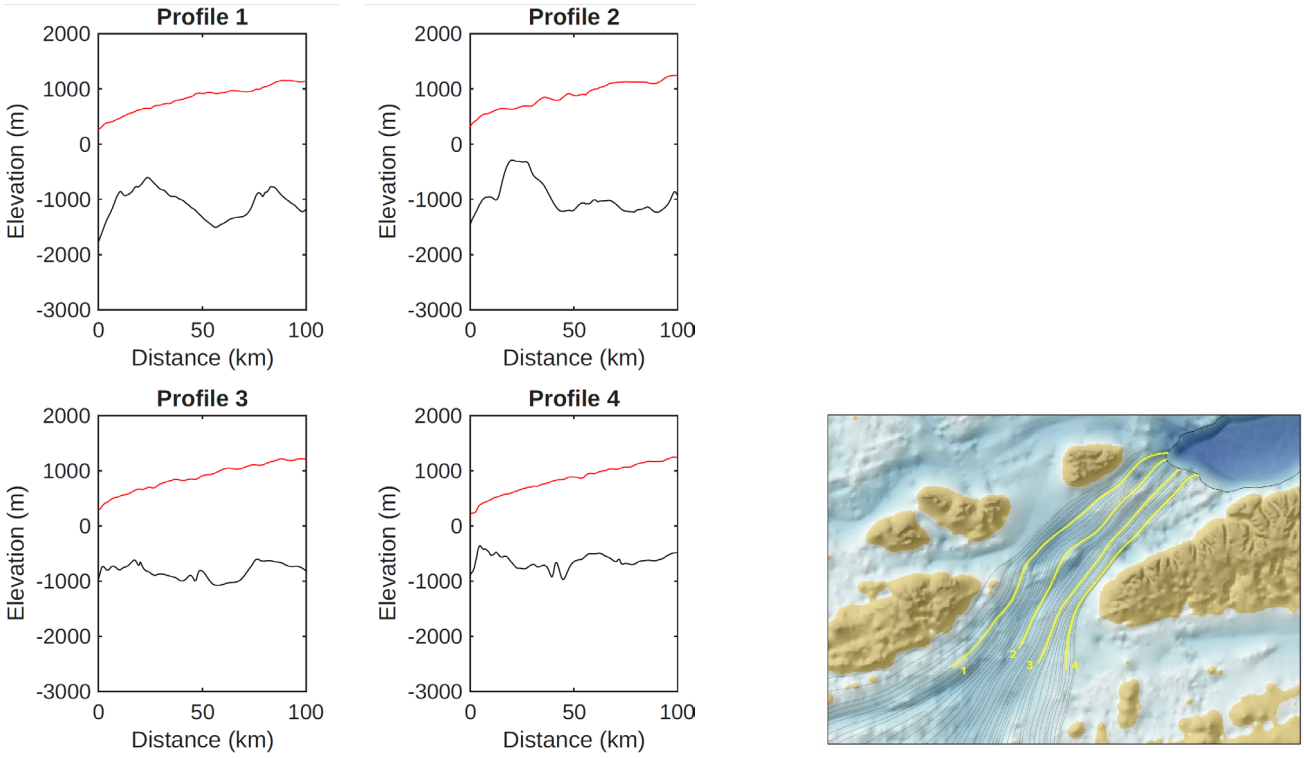

Supplementary Figure S10: Four bed and surface profiles for Lambert Glacier, East Antarctica, extending 100 km up-glacier from the grounding line, along flowlines (for locations see map in bottom right corner). The profile data and flowlines are from the Bedmap3 datasets (Pritchard et al., 2025).

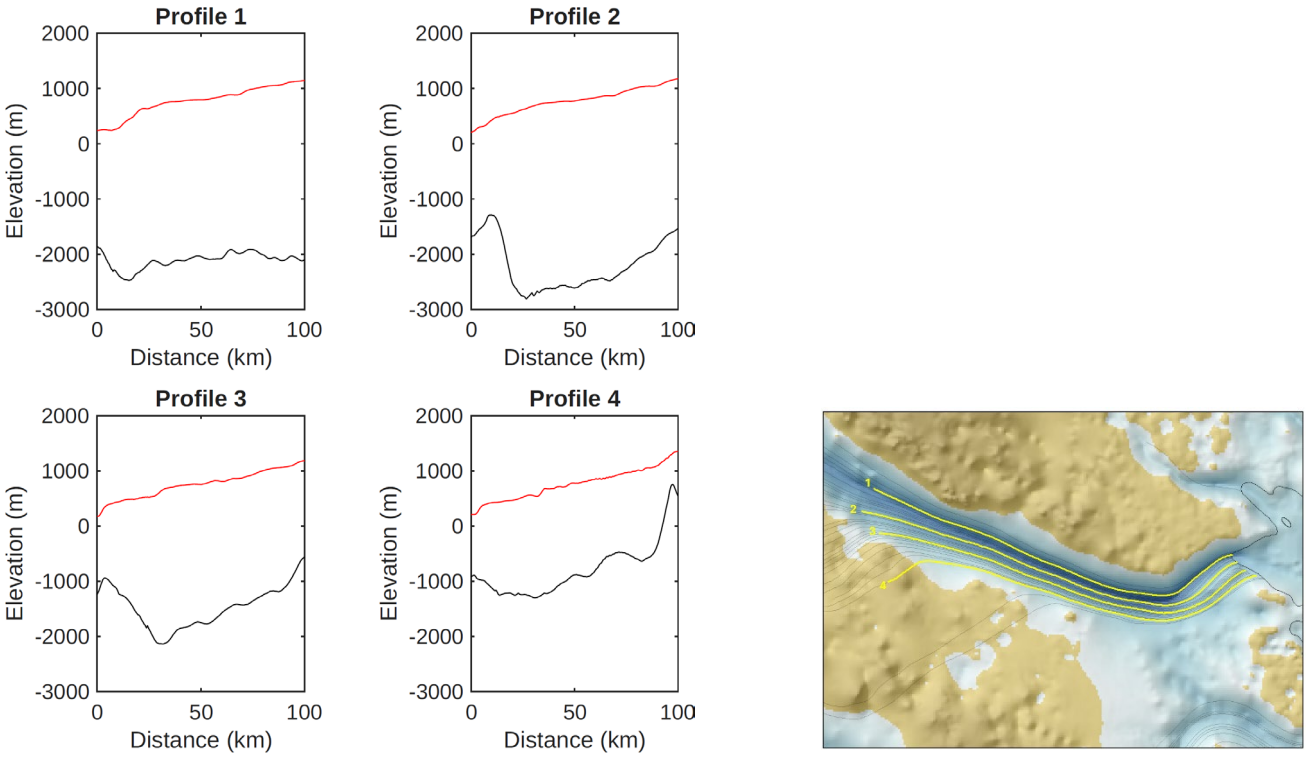

Supplementary Figure S11: Four bed and surface profiles for Denman Glacier, East Antarctica, extending 100 km up-glacier from the grounding line, along flowlines (for locations see map in bottom right corner). The profile data and flowlines are from the Bedmap3 datasets (Pritchard et al., 2025).

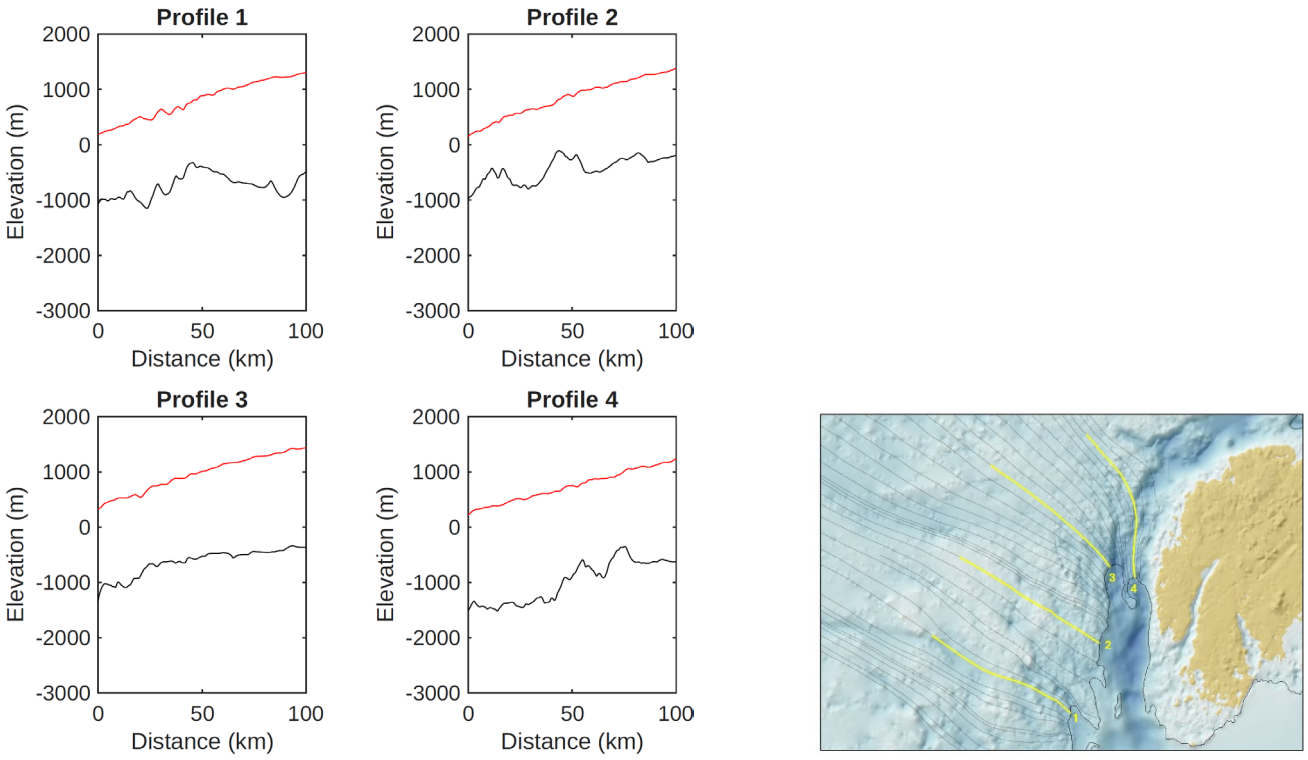

Supplementary Figure S12: Four bed and surface profiles for Totten Glacier, East Antarctica, extending 100 km up-glacier from the grounding line, along flowlines (for locations see map in bottom right corner). The profile data and flowlines are from the Bedmap3 datasets (Pritchard et al., 2025).

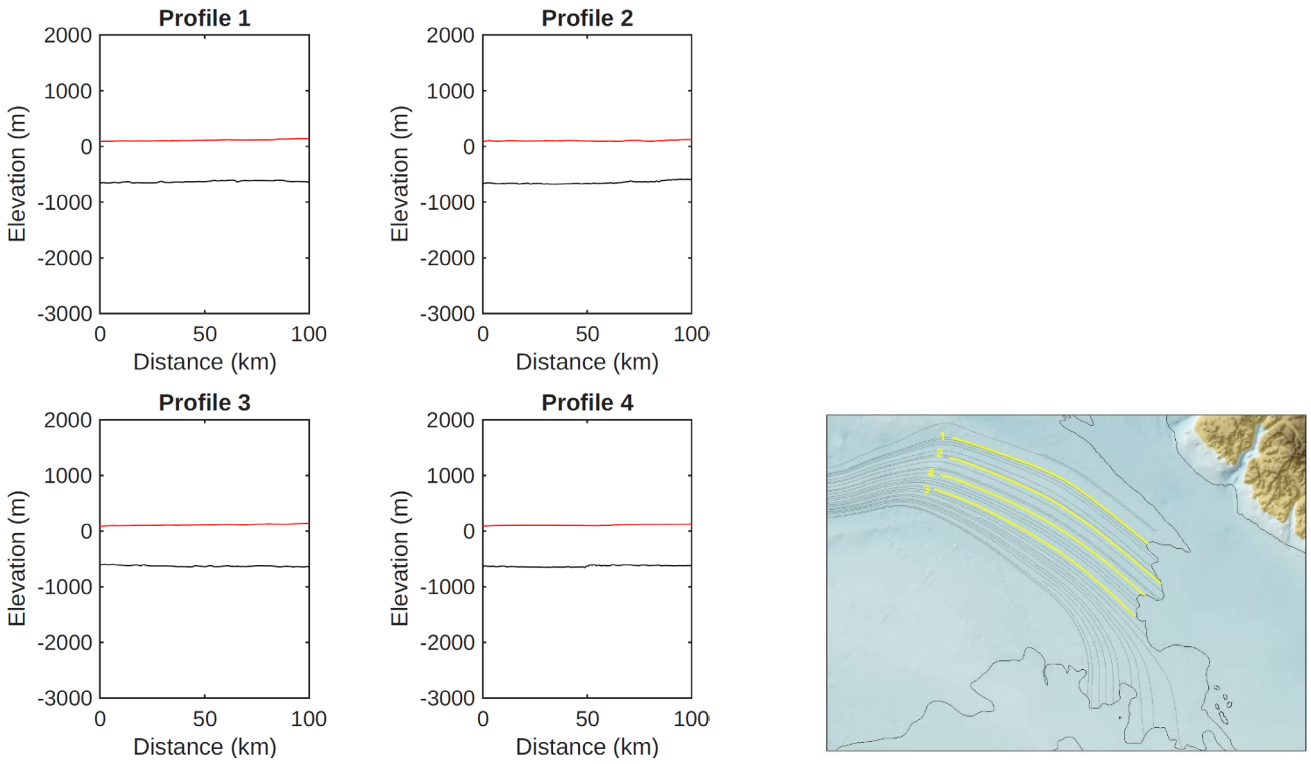

Supplementary Figure S13: Four bed and surface profiles for Whillans Ice Stream, Ross Sea, extending 100 km up-glacier from the grounding line, along flowlines (for locations see map in bottom right corner). The profile data and flowlines are from the Bedmap3 datasets (Pritchard et al., 2025).